JOURNAL OF QUATERNARY SCIENCE (2024) **39**(4) 515–530 ISSN 0267-8179. DOI: 10.1002/jqs.3605

JQS Journal of Quaternary Science QRA Quaternary Research Association

# Inherited terrestrial cosmogenic nuclides in landscapes of selective glacial erosion: lessons from Lochnagar, Eastern Grampian Mountains, Scotland

**ADRIAN M. HALL,[1]* DAVID E. SUGDEN,[1] STEVEN A. BINNIE,[2] ANDY HEIN,[1] TIBOR DUNAI,[2] BENEDIKT RITTER[2] and MARGARET STEWART[3]**

[1]Institute of Geography, School of GeoSciences, University of Edinburgh, Edinburgh, UK
[2]Institute of Geology & Mineralogy, University of Köln, Köln, Germany
[3]British Geological Survey, The Lyell Centre, Edinburgh, UK

Received 25 September 2023; Revised 25 January 2024; Accepted 1 February 2024

ABSTRACT: Inheritance from prior exposure often complicates the interpretation of terrestrial cosmogenic nuclide (TCN) inventories in glaciated terrain. Lochnagar, a mountain in eastern Scotland, holds a clear geomorphological record of corrie glaciation and the thinning of the last Scottish ice sheet over the last ~15 ka. Yet attempts to date the main stages in deglaciation after sampling of 21 granite boulders for $^{10}$Be, $^{26}$Al and $^{14}$C from corrie moraines, an ice sheet lateral moraine and boulder spreads revealed widespread, but variable, TCN inheritance. Only the youngest boulder ages fit within the range of expected deglaciation ages. To identify the sources of geological uncertainty, we provide simple models of ice cover duration and erosion histories for plateau, corrie and strath landscape domains, identify the variable nuclide inheritance that derives from different sources for boulders in these domains, and outline the effects of rotation, splitting and erosion of boulders during glacial transport. The combined effects increase clustering around arbitrary mean TCN values that exceed deglaciation ages. A further implication is that boulders have survived beneath overriding ice sheets. Such boulder trapping at Lochnagar may have resulted from topographic controls on katabatic winds and surface ablation acting on a thinning, cold-based ice sheet.


KEYWORDS: boulder transport; cosmogenic nuclide inheritance; deglaciation; enhanced ablation; glacial erosion; katabatic winds; landscape domains

## Introduction

Terrestrial cosmogenic nuclide (TCN) inventories have contributed significantly to our understanding of the exposure ages of landforms and of rates of weathering and erosion during their development. An important application is the dating of glacially transported boulders to constrain the timing of deglaciation. Multiple published datasets for boulders on moraines show a wide range of TCN concentrations (Applegate et al., 2012, Larsen et al., 2021, Çiner et al., 2017, Jena et al., 2023), indicating that the deglaciation signal is complicated by noise, or 'geological uncertainty' (Balco, 2011). Common sources of noise in boulder populations in glaciated terrains include inherited exposure (Putkonen and Swanson, 2003) and reworking (Ivy-Ochs and Kober, 2008). Furthermore, individual boulders can be exhumed, rotated, eroded and shielded through time (Gosse and Phillips, 2001, Putkonen and Swanson, 2003). Hence, TCN inventories and the derived apparent exposure ages in boulders with noise may deviate from simple inventories and true deglaciation ages. The problem of TCN inheritance and strategies for reducing noise in formerly glaciated areas have been widely discussed (Hein et al., 2014, Briner et al., 2016, Margreth et al., 2016, Larsen et al., 2021). Various statistical techniques are available for identifying mixed populations of boulders in large sample sets (Applegate et al., 2010, Dortch et al., 2022, Heyman et al., 2011, Douglass et al., 2006), but these techniques are unsuited to small datasets.

Limited consideration has been given previously to the importance of distinctive geomorphic settings or *landscape domains* for understanding geological uncertainty in boulder populations (Corbett et al., 2016, Kleman et al., 2021). Yet many studies have shown that this noise is often low in landscapes with high glacial erosion rates, such as in alpine mountain ranges (Ivy-Ochs et al., 2007), beneath valley glaciers (Schimmelpfennig et al., 2012) or under fast-flowing ice streams (Heyman et al., 2011, Corbett et al., 2011). Generally, geological uncertainty is greater in landscapes with moderate to low glacial erosion rates, particularly on plateaux (Stroeven et al., 2011, Kleman et al., 2021) and in lowland terrains (Davis et al., 2006) covered for long periods by non-erosive cold-based ice. Inheritance also tends to increase with elevation in landscapes of selective glacial erosion (Briner et al., 2006, Li et al., 2005, Stroeven et al., 2002, Skov et al., 2020, Ballantyne, 2010, Jansen et al., 2019). This makes sense because a significant thickness (~2–3 m) of rock needs to be removed by erosion in a single glaciation to reset $^{10}$Be and $^{26}$Al inventories (Fabel et al., 2004). Consequently, in landscape domains with lower depths of erosion, TCN inheritance is a major problem when seeking to establish deglaciation ages and erosion rates.

Our overall aim in this paper is to report and understand the large range and variability of cosmogenic nuclide inventories

*Correspondence: Adrian M. Hall, as above.
E-mail: adrian.hall@ed.ac.uk

in a well-studied sequence of landforms at Lochnagar in eastern Scotland. The landforms include boulder moraines that record stages in the thinning of the last ice sheet and the activity of the Lochnagar corrie glacier. The clarity of the landform record and the dominance of quartz-rich granite bedrock in the wider Cairngorms have attracted interest from the cosmogenic isotope community over the years (Kirkbride et al., 2014, Phillips et al., 2006, Everest and Kubik, 2006). In and around Lochnagar we thought we had a well-constrained geomorphology and we designed TCN sampling to fix the age of distinct landforms and stages of deglaciation. However, our $^{10}$Be, $^{26}$Al and $^{14}$C measurements on individual landforms generally exceed expected deglaciation ages, indicating widespread TCN inheritance. Here, we try to decipher the variability in TCN inventories by considering (i) contrasting exposure, burial and erosion histories in the landscape domains that were sources for the boulders, and (ii) the transport and erosion histories of individual boulders. Our results suggest that some boulders have remained trapped on the upper flanks of Lochnagar over at least two ice-sheet glaciations.

## Background

### *Landforms*

The mountain of Lochnagar (1148 m a.s.l.) is part of a granite massif that dominates the southern flanks of the valley of the Dee (Fig. 1). During the Pleistocene, successive overriding ice sheets flowed eastward down the Dee Valley towards the North Sea (Brown, 1993). The landforms of the massif (Hall, 2007) are similar to those of the Cairngorm Mountains (Gordon and Brazier, 2021) and the wider area of the east Grampians (Kirkbride, 2021). Indeed, the landform assemblages represent a classic example of a landscape of selective glacial erosion (Sugden, 1968, Hall and Glasser, 2003).

Three landscape domains can be recognized (Fig. 2; Table 1). First, the *plateaux* at higher altitudes bear tors and are blanketed and ornamented by sediments and minor landforms that developed under periglacial conditions (Phillips et al., 2006); the tors and blockfields on the Lochnagar plateau and the conical hills of Meikle Pap are shown in Fig. 3A and B. Second, *corries* backed by cliffs are incised into the plateau edge (Sugden, 1969) (Fig. 3C and D). Lochnagar corrie displays long talus slopes and two sets of arcuate boulder moraines bounding a small lake at 750 m (Clapperton, 1986, Sissons and Grant, 1972). Third, broad valleys or *straths* and steep-sided glens dissect the plateaux (Hall and Gillespie, 2016). The strath floors have thick till and glacifluvial sediment covers (Fig. 3E and F). The upper boundary of the strath domain is locally marked by glacial trimlines and lateral moraines on the flanks of the plateau.

The highest trimline on the Lochnagar massif truncates solifluction lobes at ~900 m a.s.l. on the flanks of Cuidhe Cròm (Fig. 1). On the eastern flank of this hill, a series of lateral meltwater channels descend from 810 to 650 m a.s.l. (Figs. 1, 2 and 3E) and record early thinning of the ice sheet margin. In the Lochnagar corrie embayment, a boulder lateral moraine at ~650 m marks a later margin of the Dee valley glacier (Figs. 1, 2 and 3E). Large granite boulders were originally derived from the headwall of Lochnagar corrie; the moraine does not occur west

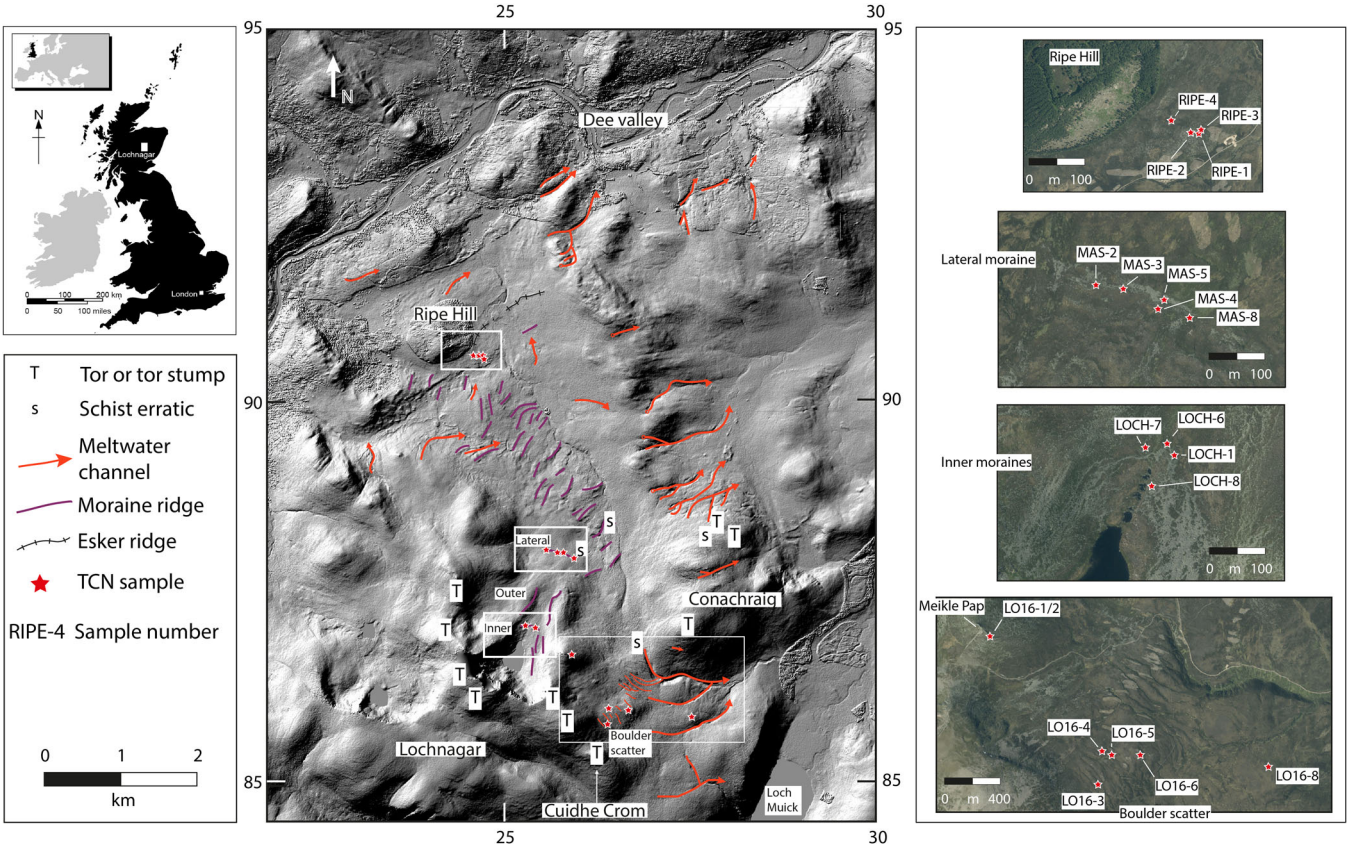


**Figure 1.** Digital Terrain Model of the ground between Lochnagar and the River Dee showing the smooth slopes of the uplands and the steeper lee slopes of large roches moutonnées in the valley floor. Meltwater channels occur in the lee of the ridge culminating in Conachcraig and reflect the eastward flow of the ice sheet. There is a concentration of depositional ridges and downslope channels on the lower ground between the corrie forefield and Ripe Hill. Locations of the TCN sample sites are given on the air photos. Intermap Technologies (2007): NEXTMap British Digital Terrain Model Dataset Produced by Intermap. NERC Earth Observation Data Centre, 2023. http://catalogue.ceda.ac.uk/uuid/8f6e1598372c058f07b0aeac2442366d. [Color figure can be viewed at wileyonlinelibrary.com]

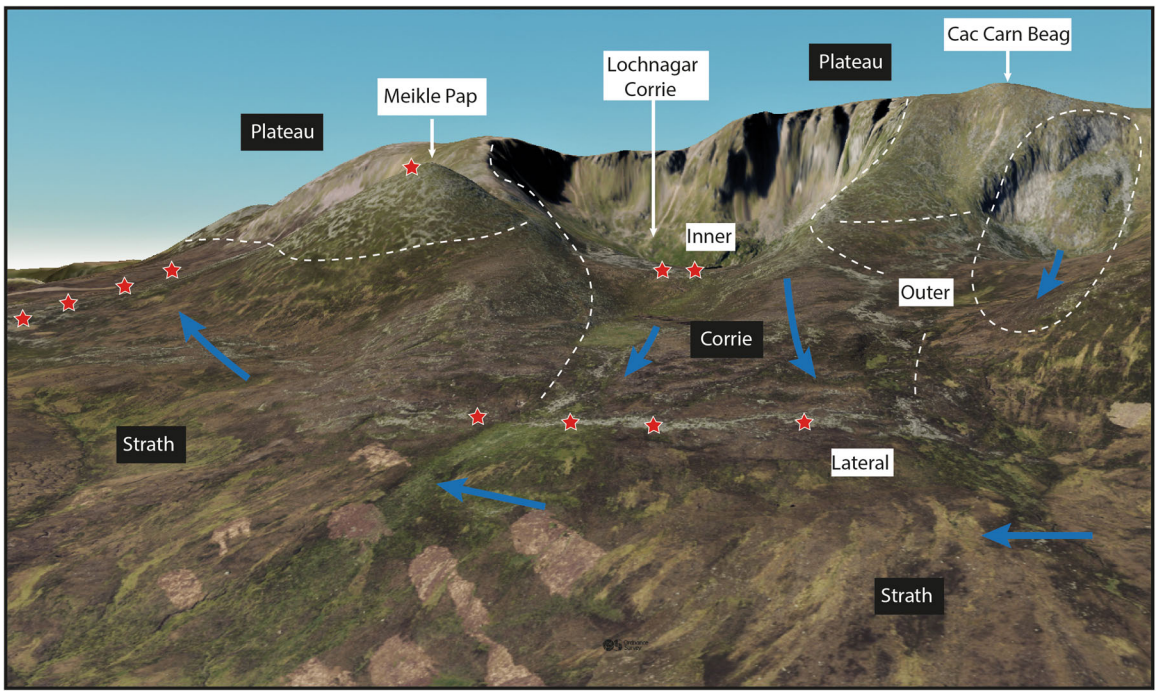


**Figure 2.** The Lochnagar massif in an oblique DTM seen from the north. Dashed lines depict the boundaries of the plateau, corrie and strath landscape domains. Stars indicate the locations of the TCN samples. Blue arrows show main ice flow directions. Ordnance Survey copyright. [Color figure can be viewed at wileyonlinelibrary.com]

**Table 1.** Landscape domains in the eastern Grampians.

| Domain name | Landform assemblage |
|---|---|
| Plateau | Tors, blockfields, mountain top detritus, weathering pits, solifluction lobes and sheets |
| Corrie | Cliffs, talus, boulder moraines |
| Strath | On gentle upper slopes, rock exposures, weak glacial roughening and streamlining, lateral meltwater channels, boulder moraines, thin till. On valley floors, strong glacial roughening and local streamlining, large roches moutonnées, meltwater channels cut in rock and sediment, moraines, till, glacifluvial deposits |

of the corrie forefield. The merging of granite boulders derived from the corrie with ice-sheet marginal landforms indicates a period of confluence between the corrie glacier and the ice sheet. Later thinning is marked by meltwater channels that cut the Conachraig ridge and by lateral moraines below 650 m which descend towards the Dee valley floor (Hall, 2007) (Fig. 1). The valley floor domain includes several large roche moutonnées, including Ripe Hill (Fig. 3F) (Sugden et al., 1992).

### *Chronology*

There is general agreement that the Scottish ice sheet was sufficiently thick and extensive to cover all the mountain summits of the east Grampians at the Last Glacial Maximum that peaked at 25–27 ka (Hughes et al., 2022). Significant thinning of the ice sheet in eastern Scotland began around 19 ka (Phillips et al., 2008) and radiocarbon dates in kettle holes show that ice had disappeared from the upper Dee Valley by 14.6 ka (Huntley, 1994) and in Abernethy Forest in Strath Spey on the northern flanks of the Cairngorms by 14.7 ka (Vasari and Vasari, 1968). In the Cairngorms, a significant readvance during ice retreat is marked along the margins of a former outlet glacier in Strath Spey by thick deposits and meltwater channels; $^{10}$Be exposure ages indicate a timing of 15.1 ± 1.1 ka (recalculated here to 15.3 ka) (Hall et al., 2016). This readvance is thought to reflect an increase in precipitation towards the end of Greenland Stadial GS-2a (16.9–14.7 ka) (Steffensen et al., 2008). It is likely that the ice-sheet lateral moraine found in a similar setting on the flanks of Lochnagar represents the termination of this readvance at 14.7 ka, although it is previously undated. Corrie glacier growth also probably occurred in the Northern Corries of the Cairngorms around this time as the ice sheet thinned (Standell, 2014, Tonkin, 2022).

There was renewed mountain glaciation in the Eastern Grampians during GS-1 (12.85–11.65 ka cal BP) (Kirkbride, 2021), including in corries in the Cairngorms (Kirkbride et al., 2014). At Loch Lomond, Scotland, the equivalent Younger Dryas glacial maximum occurred at 12.0 ka or up to 300 years later (Macleod et al., 2011). The expected age of the inner moraines at Lochnagar is 12.0 ka.

## Methods

### *TCN sampling and analysis*

In this paper we present a set of 19 new exposure ages on a sequence of lowering ice-margins on the high eastern flank of Lochnagar (Table 2). TCN samples were collected from the surface of 17 large stable boulders by hammer and chisel and, in 2016, by angle grinder. Topographic shielding was measured in the field and sample location data were collected by handheld GPS. Sample collection in 1998 was from the inner arcuate corrie moraines (LOCH-1 and LOCH-6 to LOCH-8) as well as from the granite boulders on the large ice-sheet moraine on the northern flank of Lochnagar (MAS-1 to MAS-8) (Fig. 1). These samples were processed according to

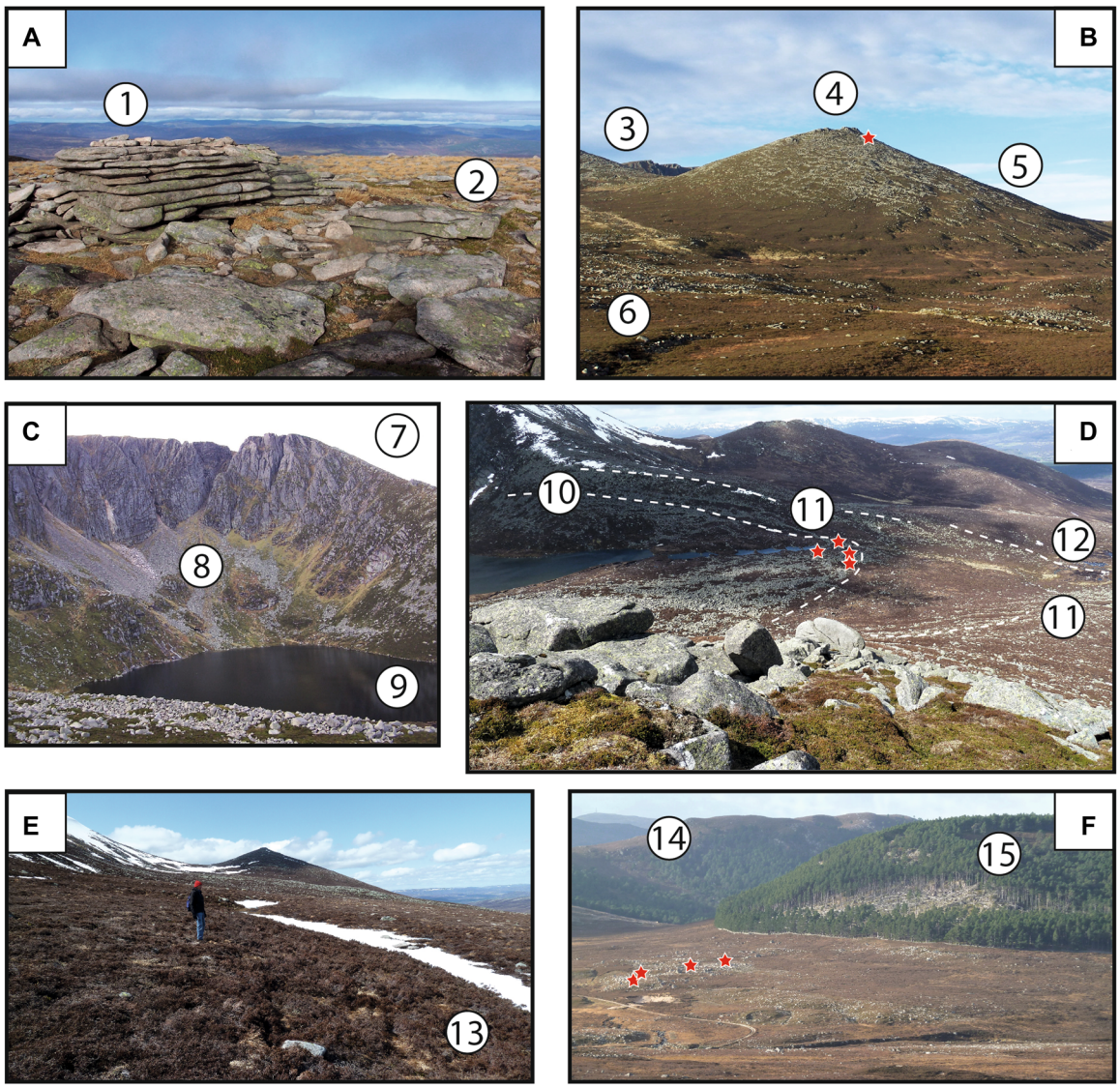


**Figure 3.** Ground photographs of the three landscape domains. (A) Small tor (1) and adjacent blockfield (2) on the summit of Cuidhe Cróm. (B) View of Meikle Pap (978 m) showing the cliff tops of Lochnagar (3), small summit tors (4), the downslope limit of solifluction lobes (5) and a lateral meltwater channel (6). The tor sample site for LO16-1 and -2 is marked by a star. (C) The cliffs of Lochnagar (7), its talus slopes (8) and the lochain (9). (D) The inner set of boulder moraines of probable Younger Dryas age (10), the limit of the outer set of boulder moraines (11) and the ice sheet lateral moraine (12). (E) Lateral meltwater channel picked out by snow (13). (F) Part of the Dee valley floor around Ripe Hill. Glacial roughening of a ridge top (14), the lee-side cliff of Ripe Hill and the location of the boulder train (16). Stars indicate the locations of the TCN samples. [Color figure can be viewed at wileyonlinelibrary.com]

protocols at the Scottish Universities Research and Reactor Centre (SUERC) at East Kilbride and measured by accelerator mass spectrometry (AMS) at the ETH Zurich AMS facility. Other samples were collected in 2016 from a small tor (LO16-1 to -2) and from boulder spreads (LO16-3 to -8) east of Lochnagar corrie (Fig. 1). The latter samples were processed according to protocols at the University of Cologne (Binnie et al., 2015). Procedures are described in Hall et al. (2016) for the measurements of $^{10}$Be and $^{26}$Al and follow Fülöp et al. (2015) for the derivation of $^{14}$C concentrations. AMS measurements were made on CologneAMS (Dewald et al., 2013, Schiffer et al., 2020) using splits of the same purified quartz for $^{14}$C in which $^{10}$Be and $^{26}$Al were determined. Finally, we include discussion of four published dates on a boulder train in the lee of Ripe Hill near the floor of the Dee Valley (RIPE-1 to RIPE-4). The procedures and protocols for the latter are described in Sugden et al. (2019).

For consistency in this paper, we have standardized all exposure ages using the online exposure age calculator formerly known as the CRONUS-Earth online exposure age calculator, Version 3 (Balco et al., 2008) with local $^{10}$Be, $^{26}$Al and $^{14}$C production rates for Scotland (Borchers et al., 2016). Reported ages use the LSDn (Lifton et al., 2014) scaling model with no snow cover or erosion rate correction, and thus are minimum ages. We prefer to use LSD scaling over other schemes as it caters for magnetic field variations over time and is based on first principle particle physics rather than fits to proxy datasets. The results for other scaling schemes are given in Table 3. Raw data used for calculating nuclide concentrations are given in Table S1. Uncertainties are given at 1-sigma throughout. An erosion rate of 1.6 mm ka$^{-1}$ was reported for the Cairngorms based on the measurement of raised quartz veins (Phillips et al., 2006); we demonstrate the effect of this erosion rate on our samples in Table 3. We obtained paired $^{10}$Be and $^{26}$Al isotope data for samples LO16-1 to LO16-8. Data were plotted using the iceTEA tool (http://ice-tea.org) (Jones et al., 2019). $^{14}$C data are reported for LO16-3 to -8. Published data for Coire an't Lochain (Kirkbride et al., 2014) and a lateral moraine in the Northern Cairngorms (Hall et al., 2016) are recalibrated in the same way for consistency.

**Table 2.** Rock sample details and cosmogenic nuclide concentrations in quartz-bearing granite rocks, Lochnagar, East Grampians, Scotland.

| Sample ID | Lat. (DD) | Long. (DD) | Elevation (m) | Qtz mass (g) | Pressure flag | Thickness (cm) | Density (g cm$^{-3}$) | Topo shielding corr. | Erosion rate (cm a$^{-1}$) | Year collected | Sample ID | Isotope | Mineral | Concentration (at. per g $SiO_2$) | ±1σ | Standard |
|---|---|---|---|---|---|---|---|---|---|---|---|---|---|---|---|---|
| LO16-1[a] | 56.9608 | −3.2166 | 951 | | std | 0.5 | 2.6 | 0.9910 | 0 | 2016 | LO16-1a | $^{10}$Be | Quartz | 2.9862E+05 | 1.0428E+04 | 07KNSTD |
| | | | | | | | | | | | LO16-1 | $^{26}$Al | Quartz | 2.2307E+06 | 1.4137E+05 | KNSTD |
| | | | | | | | | | | | LO16-1 | $^{14}$C | Quartz | 2.7531E+05 | 4.3676E+03 | |
| LO16-2[a] | 56.9591 | −3.2168 | 947 | | std | 2 | 2.6 | 0.9968 | 0 | 2016 | LO16-2a | $^{10}$Be | Quartz | 6.2855E+05 | 2.1140E+04 | 07KNSTD |
| | | | | | | | | | | | LO16-2 | $^{26}$Al | Quartz | 4.2349E+06 | 2.4672E+05 | KNSTD |
| | | | | | | | | | | | LO16-2 | $^{14}$C | Quartz | 2.6917E+05 | 4.4272E+03 | |
| LO16-3[a] | 56.9504 | −3.2051 | 801 | | std | 1.5 | 2.6 | 0.9950 | 0 | 2016 | LO16-3a | $^{10}$Be | Quartz | 1.5950E+05 | 5.8737E+03 | 07KNSTD |
| | | | | | | | | | | | LO16-3 | $^{26}$Al | Quartz | 9.4649E+05 | 9.1259E+04 | KNSTD |
| | | | | | | | | | | | LO16-3 | $^{14}$C | Quartz | 2.7998E+05 | 4.3004E+03 | |
| LO16-4[a] | 56.9525 | −3.2044 | 781 | | std | 1 | 2.6 | 0.9971 | 0 | 2016 | LO16-4a | $^{10}$Be | Quartz | 2.1651E+05 | 7.7153E+03 | 07KNSTD |
| | | | | | | | | | | | LO16-4 | $^{26}$Al | Quartz | 1.4103E+06 | 8.9975E+04 | KNSTD |
| LO16-5[a] | 56.9525 | −3.2044 | 781 | | std | 1 | 2.6 | 0.9971 | 0 | 2016 | LO16-5a | $^{10}$Be | Quartz | 2.2552E+05 | 7.9466E+03 | 07KNSTD |
| | | | | | | | | | | | LO16-5 | $^{26}$Al | Quartz | 1.2332E+06 | 1.2335E+05 | KNSTD |
| LO16-6[a] | 56.9520 | −3.2000 | 762 | | std | 1.5 | 2.6 | 0.9979 | 0 | 2016 | LO16-6a | $^{10}$Be | Quartz | 1.6096E+05 | 5.8944E+03 | 07KNSTD |
| | | | | | | | | | | | LO16-6 | $^{26}$Al | Quartz | 9.9205E+05 | 9.4856E+04 | KNSTD |
| | | | | | | | | | | | LO16-6 | $^{14}$C | Quartz | 2.7420E+05 | 5.4673E+03 | |
| LO16-7[a] | 56.9543 | −3.1907 | 681 | | std | 2 | 2.6 | 0.9989 | 0 | 2016 | LO16-7a | $^{10}$Be | Quartz | 4.7518E+05 | 1.6410E+04 | 07KNSTD |
| | | | | | | | | | | | LO16-7 | $^{26}$Al | Quartz | 2.2460E+06 | 1.2155E+05 | KNSTD |
| | | | | | | | | | | | LO16-7 | $^{14}$C | Quartz | 2.1099E+05 | 4.3634E+03 | |
| LO16-8[a] | 56.9512 | −3.1844 | 672 | | std | 1 | 2.6 | 0.9991 | 0 | 2016 | LO16-8a | $^{10}$Be | Quartz | 1.3385E+05 | 5.0905E+03 | 07KNSTD |
| | | | | | | | | | | | LO16-8 | $^{26}$Al | Quartz | 8.5520E+05 | 8.6287E+04 | KNSTD |
| | | | | | | | | | | | LO16-8 | $^{14}$C | Quartz | 2.8304E+05 | 5.2967E+03 | |
| RIPE-1[b] | 57.0028 | −3.2415 | 406 | 26.522 | std | 4 | 2.6 | 0.9942 | 0 | 2003 | RIPE-1b | $^{10}$Be | Quartz | 8.6620E+04 | 6.8180E+03 | S555 |
| RIPE-2[b] | 57.0029 | −3.2418 | 404 | 21.993 | std | 3 | 2.6 | 0.9942 | 0 | 2003 | RIPE-2b | $^{10}$Be | Quartz | 8.8932E+04 | 6.5770E+03 | S555 |
| RIPE-3[b] | 57.0029 | −3.2414 | 402 | 31.488 | std | 4 | 2.6 | 0.9942 | 0 | 2003 | RIPE-3b | $^{10}$Be | Quartz | 1.0550E+05 | 6.7770E+03 | S555 |
| RIPE-4[b] | 57.0033 | −3.2438 | 406 | 31.718 | std | 3.5 | 2.6 | 0.9942 | 0 | 2003 | RIPE-4b | $^{10}$Be | Quartz | 1.0050E+05 | 6.1620E+03 | S555 |
| LOCH-1[c] | 56.9640 | −3.2267 | 784 | 38.161 | std | 4 | 2.6 | 0.9753 | 0 | 1998 | LOCH-1c | $^{10}$Be | Quartz | 1.1930E+05 | 6.3140E+03 | S555 |
| LOCH-6[c] | 56.9646 | −3.2271 | 768 | 34.679 | std | 2.5 | 2.6 | 0.9753 | 0 | 1998 | LOCH-6c | $^{10}$Be | Quartz | 1.3145E+05 | 7.2040E+03 | S555 |
| LOCH-7[c] | 56.9643 | −3.2286 | 773 | 36.563 | std | 2 | 2.6 | 0.9753 | 0 | 1998 | LOCH-7c | $^{10}$Be | Quartz | 1.5297E+05 | 8.2180E+03 | S555 |
| LOCH-8[c] | 56.9631 | −3.2277 | 790 | 34.565 | std | 4 | 2.6 | 0.9753 | 0 | 1998 | LOCH-8c | $^{10}$Be | Quartz | 1.0456E+05 | 6.8650E+03 | S555 |
| MAS-1[c] | 56.9733 | −3.2220 | 657 | 32.400 | std | 5.5 | 2.6 | 0.9863 | 0 | 1998 | MAS-1c | $^{10}$Be | Quartz | 1.3828E+05 | 9.5100E+03 | S555 |
| MAS-2[c] | 56.9733 | −3.2243 | 655 | 30.030 | std | 7 | 2.6 | 0.9863 | 0 | 1998 | MAS-2c | $^{10}$Be | Quartz | 2.1705E+05 | 1.6588E+04 | S555 |
| MAS-3[c] | 56.9731 | −3.2224 | 652 | 29.900 | std | 5.5 | 2.6 | 0.9863 | 0 | 1998 | MAS-3c | $^{10}$Be | Quartz | 1.5427E+05 | 1.4496E+04 | S555 |
| MAS-4[c] | 56.9726 | −3.2209 | 654 | 28.660 | std | 5 | 2.6 | 0.9863 | 0 | 1998 | MAS-4c | $^{10}$Be | Quartz | 2.1697E+05 | 1.6288E+04 | S555 |
| MAS-5[c] | 56.9728 | −3.2205 | 652 | 33.100 | std | 4 | 2.6 | 0.9863 | 0 | 1998 | MAS-5c | $^{10}$Be | Quartz | 1.6773E+05 | 1.3865E+04 | S555 |
| MAS-7[c] | 56.9727 | −3.2198 | 652 | 38.700 | std | 2 | 2.6 | 0.9863 | 0 | 1998 | MAS-7c | $^{10}$Be | Quartz | 1.2141E+05 | 9.8110E+03 | S555 |
| MAS-8[c] | 56.9720 | −3.2190 | 649 | 31.480 | std | 4 | 2.6 | 0.9863 | 0 | 1998 | MAS-8c | $^{10}$Be | Quartz | 1.7350E+05 | 1.7174E+04 | S555 |

The concentrations have been corrected for process blanks; uncertainties include propogated AMS sample/lab-blank uncertainty and a 2% $^{9}$Be carrier mass uncertainty and 3% stable Al (ICP-OES) uncertainty.
[a]Chemistry and AMS measurements conducted at the University of Cologne and CologneAMS, Cologne, Germany.
[b]Originally published by Sugden et al. (2019). Chemistry completed at the University of Edinburgh, Edinburgh, UK. AMS measurements conducted at SUERC AMS, East Kilbride, UK.
[c]Chemistry completed at the University of Edinburgh, Edinburgh, UK. AMS measurements conducted at ETH Zurich, Switzerland.
All samples were spiked with ~0.25 mg $^{9}$Be carrier except for the MAS samples, which were spiked with ~0.30 mg $^{9}$Be carrier. Samples measured for $^{26}$Al were spiked with up to 1.5 g $^{27}$Al carrier depending on the native Al content.

**Table 3.** Apparent cosmogenic nuclide exposure ages in quartz-bearing granite rocks, Lochnagar, East Grampians, Scotland.

| Sample ID | Elevation (m) | Isotope | Age St scaling (ka) | ±1σ (internal) | ±1σ (external) | Age Lm scaling (ka) | ±1σ (internal) | ±1σ (external) | Age LSDn scaling (ka) | ±1σ (internal) | ±1σ (external) | Age LSDn 1 mm $ka^{-1}$ erosion (ka) | ±1σ (internal) | ±1σ (external) | Age LSDn 1.6 mm $ka^{-1}$ erosion (ka) | ±1σ (internal) | ±1σ (external) |
|---|---|---|---|---|---|---|---|---|---|---|---|---|---|---|---|---|---|
| LO16-1 | 951 | $^{10}$Be | 28.6 | 1.0 | 1.6 | 28.4 | 1.0 | 1.6 | 28.3 | 1.0 | 1.6 | 29.0 | 1.0 | 1.6 | 29.4 | 1.1 | 1.7 |
| | | $^{26}$Al | 28.6 | 1.8 | 2.8 | 28.5 | 1.8 | 2.8 | 28.5 | 1.8 | 2.8 | 29.2 | 1.9 | 3.0 | 29.6 | 2.0 | 3.1 |
| | | $^{14}$C | 27.3 | 3.4 | 36.8 | 27.3 | 3.4 | 36.9 | 29.0 | 4.2 | 45.3 | 32.7 | 7.0 | 74.5 | 36.4 | 11.4 | 121.2 |
| LO16-2 | 947 | $^{10}$Be | 61.2 | 2.1 | 3.4 | 61.0 | 2.1 | 3.3 | 60.9 | 2.1 | 3.3 | 64.0 | 2.3 | 3.7 | 66.2 | 2.5 | 3.9 |
| | | $^{26}$Al | 55.5 | 3.3 | 5.4 | 55.3 | 3.3 | 5.4 | 55.5 | 3.3 | 5.4 | 58.2 | 3.7 | 6.0 | 60.0 | 3.9 | 6.4 |
| | | $^{14}$C | 24.7 | 2.6 | 26.7 | 24.8 | 2.6 | 26.8 | 26.0 | 3.0 | 31.0 | 28.2 | 4.1 | 42.3 | 29.9 | 5.2 | 54.0 |
| LO16-3 | 801 | $^{10}$Be | 17.4 | 0.6 | 1.0 | 17.4 | 0.6 | 1.0 | 17.4 | 0.6 | 1.0 | 17.6 | 0.7 | 1.0 | 17.8 | 0.7 | 1.0 |
| | | $^{26}$Al | 13.7 | 1.3 | 1.7 | 13.8 | 1.3 | 1.7 | 13.8 | 1.3 | 1.7 | 14.0 | 1.4 | 1.7 | 14.1 | 1.4 | 1.8 |
| | | $^{14}$C | Saturated | | | Saturated | | | Saturated | | | Saturated | | | Saturated | | |
| LO16-4 | 781 | $^{10}$Be | 23.9 | 0.9 | 1.3 | 23.8 | 0.9 | 1.3 | 23.8 | 0.9 | 1.3 | 24.3 | 0.9 | 1.4 | 24.6 | 0.9 | 1.4 |
| | | $^{26}$Al | 20.8 | 1.3 | 2.1 | 20.8 | 1.3 | 2.0 | 20.8 | 1.3 | 2.1 | 21.2 | 1.4 | 2.1 | 21.4 | 1.4 | 2.2 |
| LO16-5 | 781 | $^{10}$Be | 24.9 | 0.9 | 1.4 | 24.8 | 0.9 | 1.4 | 24.8 | 0.9 | 1.4 | 25.3 | 0.9 | 1.4 | 25.6 | 0.9 | 1.5 |
| | | $^{26}$Al | 18.2 | 1.8 | 2.3 | 18.1 | 1.8 | 2.3 | 18.2 | 1.8 | 2.3 | 18.5 | 1.9 | 2.4 | 18.7 | 1.9 | 2.4 |
| LO16-6 | 762 | $^{10}$Be | 18.1 | 0.7 | 1.0 | 18.1 | 0.7 | 1.0 | 18.1 | 0.7 | 1.0 | 18.4 | 0.7 | 1.0 | 18.5 | 0.7 | 1.1 |
| | | $^{26}$Al | 14.9 | 1.4 | 1.8 | 14.9 | 1.4 | 1.8 | 15.0 | 1.4 | 1.8 | 15.1 | 1.5 | 1.9 | 15.3 | 1.5 | 1.9 |
| | | $^{14}$C | Saturated | | | Saturated | | | Saturated | | | Saturated | | | Saturated | | |
| LO16-7 | 681 | $^{10}$Be | 58.1 | 2.0 | 3.2 | 57.9 | 2.0 | 3.2 | 58.1 | 2.0 | 3.2 | 61.0 | 2.2 | 3.5 | 62.9 | 2.4 | 3.8 |
| | | $^{26}$Al | 36.7 | 2.0 | 3.4 | 36.5 | 2.0 | 3.4 | 36.7 | 2.0 | 3.5 | 37.8 | 2.2 | 3.7 | 38.5 | 2.2 | 3.8 |
| | | $^{14}$C | 21.0 | 2.0 | 16.5 | 21.0 | 2.0 | 16.5 | 21.9 | 2.2 | 18.4 | 23.0 | 2.7 | 21.8 | 23.8 | 3.0 | 24.5 |
| LO16-8 | 672 | $^{10}$Be | 16.2 | 0.6 | 0.9 | 16.2 | 0.6 | 0.9 | 16.2 | 0.6 | 0.9 | 16.4 | 0.6 | 0.9 | 16.6 | 0.6 | 1.0 |
| | | $^{26}$Al | 13.8 | 1.4 | 1.7 | 13.8 | 1.4 | 1.7 | 13.9 | 1.4 | 1.8 | 14.1 | 1.4 | 1.8 | 14.1 | 1.5 | 1.8 |
| | | $^{14}$C | Saturated | | | Saturated | | | Saturated | | | Saturated | | | Saturated | | |
| RIPE-1 | 406 | $^{10}$Be | 12.5 | 1.0 | 1.1 | 12.5 | 1.0 | 1.1 | 12.6 | 1.0 | 1.1 | 12.7 | 1.0 | 1.1 | 12.8 | 1.0 | 1.2 |
| RIPE-2 | 404 | $^{10}$Be | 12.8 | 0.9 | 1.1 | 12.8 | 0.9 | 1.1 | 12.8 | 1.0 | 1.1 | 13.0 | 1.0 | 1.1 | 13.0 | 1.0 | 1.1 |
| RIPE-3 | 402 | $^{10}$Be | 15.3 | 1.0 | 1.2 | 15.3 | 1.0 | 1.2 | 15.4 | 1.0 | 1.2 | 15.5 | 1.0 | 1.2 | 15.7 | 1.0 | 1.2 |
| RIPE-4 | 406 | $^{10}$Be | 14.5 | 0.9 | 1.1 | 14.5 | 0.9 | 1.1 | 14.5 | 0.9 | 1.1 | 14.7 | 0.9 | 1.1 | 14.8 | 0.9 | 1.1 |
| LOCH-1 | 784 | $^{10}$Be | 12.5 | 0.7 | 0.8 | 12.5 | 0.7 | 0.8 | 12.5 | 0.7 | 0.8 | 12.7 | 0.7 | 0.9 | 12.7 | 0.7 | 0.9 |
| LOCH-6 | 768 | $^{10}$Be | 13.8 | 0.8 | 1.0 | 13.8 | 0.8 | 1.0 | 13.8 | 0.8 | 1.0 | 14.0 | 0.8 | 1.0 | 14.1 | 0.8 | 1.0 |
| LOCH-7 | 773 | $^{10}$Be | 15.9 | 0.9 | 1.1 | 15.9 | 0.9 | 1.1 | 16.0 | 0.9 | 1.1 | 16.2 | 0.9 | 1.1 | 16.3 | 0.9 | 1.1 |
| LOCH-8 | 790 | $^{10}$Be | 10.9 | 0.7 | 0.9 | 10.9 | 0.7 | 0.9 | 10.9 | 0.7 | 0.9 | 11.0 | 0.7 | 0.9 | 11.1 | 0.7 | 0.9 |
| MAS-1 | 657 | $^{10}$Be | 16.2 | 1.1 | 1.3 | 16.2 | 1.1 | 1.3 | 16.3 | 1.1 | 1.3 | 16.5 | 1.2 | 1.4 | 16.6 | 1.2 | 1.4 |
| MAS-2 | 655 | $^{10}$Be | 25.9 | 2.0 | 2.3 | 25.8 | 2.0 | 2.3 | 25.8 | 2.0 | 2.3 | 26.4 | 2.1 | 2.4 | 26.7 | 2.1 | 2.4 |
| MAS-3 | 652 | $^{10}$Be | 18.2 | 1.7 | 1.9 | 18.2 | 1.7 | 1.9 | 18.2 | 1.7 | 1.9 | 18.5 | 1.8 | 1.9 | 18.7 | 1.8 | 2.0 |
| MAS-4 | 654 | $^{10}$Be | 25.5 | 1.9 | 2.2 | 25.4 | 1.9 | 2.2 | 25.4 | 1.9 | 2.2 | 26.0 | 2.0 | 2.3 | 26.3 | 2.1 | 2.4 |
| MAS-5 | 652 | $^{10}$Be | 19.5 | 1.6 | 1.8 | 19.5 | 1.6 | 1.8 | 19.6 | 1.6 | 1.8 | 19.9 | 1.7 | 1.9 | 20.1 | 1.7 | 1.9 |
| MAS-7 | 652 | $^{10}$Be | 13.9 | 1.1 | 1.3 | 13.9 | 1.1 | 1.3 | 14.0 | 1.1 | 1.3 | 14.1 | 1.2 | 1.3 | 14.2 | 1.2 | 1.3 |
| MAS-8 | 649 | $^{10}$Be | 20.3 | 2.0 | 2.2 | 20.2 | 2.0 | 2.2 | 20.3 | 2.0 | 2.2 | 20.6 | 2.1 | 2.3 | 20.8 | 2.1 | 2.3 |

Exposure ages calculated using the exposure age calculator formerly known as the CRONUS-Earth online exposure age calculator (Balco et al. (2008), version 3.0: Wrapper script 3.0.2, muons 1A, constants 2020-08-26; accessed April 2023. Ages calculated with local $^{10}$Be, $^{26}$Al and $^{14}$C production rates for Scotland described by Borchers et al. (2016). Exposure ages are reported based on three scaling schemes: St-scaling [Lal (1991) revised by Stone (2000)], Lm-scaling [Time-dependent Lal/Stone] and LSDn-scaling [Lifton et al., 2014]. Unless otherwise indicated, exposure ages assume no rock surface erosion or shielding by snow, and thus are minimum ages.

### Conceptual model of exposure and burial history

To interpret TCN inheritance of a sample it is necessary to understand the exposure and burial history of that sample. We present a model of ice cover in the plateau, corrie and strath domains during the last glacial cycle (Fig. 5) based on extrapolation of the oxygen isotope record in the North GRIP ice core from the Greenland Ice Sheet (Merritt et al., 2019). Following Clapperton (1997), we use a threshold $\delta^{18}O$ oxygen isotope value permitting corrie glaciation at 37‰. The threshold for an ice sheet is a $\delta^{18}O$ oxygen isotope value ≥40.5‰. Shielding ice and thick snow are assumed to cover the plateau during both corrie and ice sheet glaciation. When discussing exposure–burial models, we ignore the decay of $^{10}Be$ during burial because its half-life ($1.39 \times 10^6$ years) is large compared to the relatively short (tens of thousands of years) burial periods considered.

### Corrie boulder creation rates

Granite boulders derived by rockfall from the headwall and sidewall of the Lochnagar corrie are found in arcuate moraine ridges in the corrie forefield. The boulder volumes allow first-order estimates to be derived for rates of boulder release from the corrie walls. It is assumed that no boulders are sourced from bedrock on the corrie floor because no bedrock is exposed here today. The rock volumes are calculated for boulders held in the inner and outer sets of corrie moraines. The total volume of the moraine ridges is estimated from the area of the ridges in digital elevation models (DEMs), with assumed moraine depths of 2 m and a porosity of 50%. Boulder creation rates are derived using the duration of the Younger Dryas stadial (1.2 ka) for the inner moraine ridges (Kirkbride, 2006). Application of the estimated rockfall retreat rate to the total headward retreat of the corrie headwall loosely constrains the time required to erode Lochnagar corrie.

## Results

Apparent $^{10}Be$ and $^{26}Al$ exposure ages from various studies of Lochnagar are given in Tables 2 and 3. Below we describe the results in relation to landscape domains.

### Plateau domain

Two samples were taken from bedrock on the small tor on Meikle Pap at an elevation of around 940 m a.s.l. (LO16-1, LO16-2) (Fig. 1 and Table 2). The upper tor surface is marked by variously weathered granite sheets aligned parallel to joints and to the surrounding slope (Fig. 4). In places the upper sheeting is absent and exposes a more coherent base. LO16-2 was taken from the surface of an uppermost, sloping 0.5-m-thick sheet of granite. LO16-1 was sampled from an immediately adjacent bedrock step missing the upper sheet (Fig. 4). We interpret the upper sheet as part of the undisturbed tor and the loss of a nearby rock sheet as due to erosion. Similar block loss after glacial entrainment is reported from tors in the Cairngorms (Hall and Phillips, 2006a).

The uppermost sample from the top of the sheet (LO16-2) yielded an apparent $^{10}Be$ exposure age of 60.9 ka and that of the adjacent lower step (LO16-1) of 28.3 ka. Restoration of a 0.5 m thickness of rock above the lower sample, equivalent to the estimated thickness of the lost slab, generates pre-slab loss TCN inventory which is equivalent to that held in the undisturbed upper sample. This is consistent with removal of the slab from the tor during the last glaciation.

### Corrie domain

Four samples were taken from the inner set of arcuate boulder moraines in Lochnagar corrie at elevations of 770–790 m (Loch-1, Loch-6 to -8) (Figs. 1 and 4). The $^{10}Be$ exposure ages range from 10.9 to 16.0 ka (Table 3). Only one boulder age (Loch-1: $12.5 \pm 0.9$ ka) is within error of the expected deglaciation age of 12.0 ka (Macleod et al., 2011).

### Strath domain

The initial attempt to date the wastage of the last ice sheet was focused on the lateral boulder moraine at ~650 m (Figs. 1 and 2). Seven large granite boulders were sampled from the crest of the moraine (MAS-1 to -5, MAS-7 to -8) (Fig. 4). The $^{10}Be$ apparent ages are 14.1–26.1 ka. Three boulders had exposure ages over ~20 ka. Only the youngest age of 14.1 ka approximates to the expected deglaciation age of 14.7 ka.

A subsequent attempt was made to sample isolated, large boulders spread across a clear sequence of higher ice-sheet margins represented by ridges and lateral meltwater channels at elevations of 810–660 m (Figs. 1, 2 and 4). This vertical transect represents the thinning of a coherent ice sheet before it became confined to the Dee and Muick valleys. In declining order of altitude and timing of deposition during ice thinning the apparent $^{10}Be$ exposure ages (LO16-3 to -8) are highly variable: 17.4, 23.8, 24.8, 18.1, 58.1 and 16.2 ka (Table 3). The lowest and youngest apparent age is outside the error for the expected 14.7 ka deglaciation age at this elevation.

Measurements of $^{26}Al$ and *in situ* $^{14}C$ potentially provide additional information on the exposure and burial histories of the boulders (Table 3). The ratio of $^{26}Al/^{10}Be$ to $^{10}Be$ concentration indicates that several boulders (LO16-3 to LO16-8) or their bedrock sources may have burial histories amounting to several hundreds of thousands of years (~180–800 ka), which suggests they survived multiple glacial cycles (Fig. 5). The $^{14}C$ results indicate saturation or near saturation of the samples, which suggests the boulders have been exposed for at least ~20 ka assuming no rock surface erosion, or less if the rock is eroding. These exposure durations exceed the ~15 ka of post-glacial exposure from independent evidence and are unexpected, given a $^{14}C$ half-life of 5730 ka and prior ice cover of ~20 ka during Marine Isotope Stage (MIS) 3/2.

A different approach was to sample a boulder train close to the Dee valley floor (Fig. 1). The clear relationship between the boulder train and its source in a cliff in the lee of a large roche moutonnée at Ripe Hill (Fig. 4) would be expected to yield a firm indication of the age of the last stage of deglaciation (Sugden et al., 2019). We sampled four boulders in the train (Fig. 1: RIPE-1 to -4) and the $^{10}Be$ exposure ages range from 12.6 to 15.4 ka (mean $13.8 \pm 1.2$ ka), compared to an expected deglaciation age of 14.7 ka.

### Comparisons with similar domains in the Cairngorms

In the plateau domain on the Cairngorms, TCN ages are available for tors and for boulders glacially transported from tors. The range of published apparent $^{10}Be$ exposure ages ($n = 24$) for tors is 21–200 ka, with the greatest ages from the summits of large tors. The tor boulders range in apparent ages from 15 to 40 ka (Fig. 6), similar to apparent ages for small tors

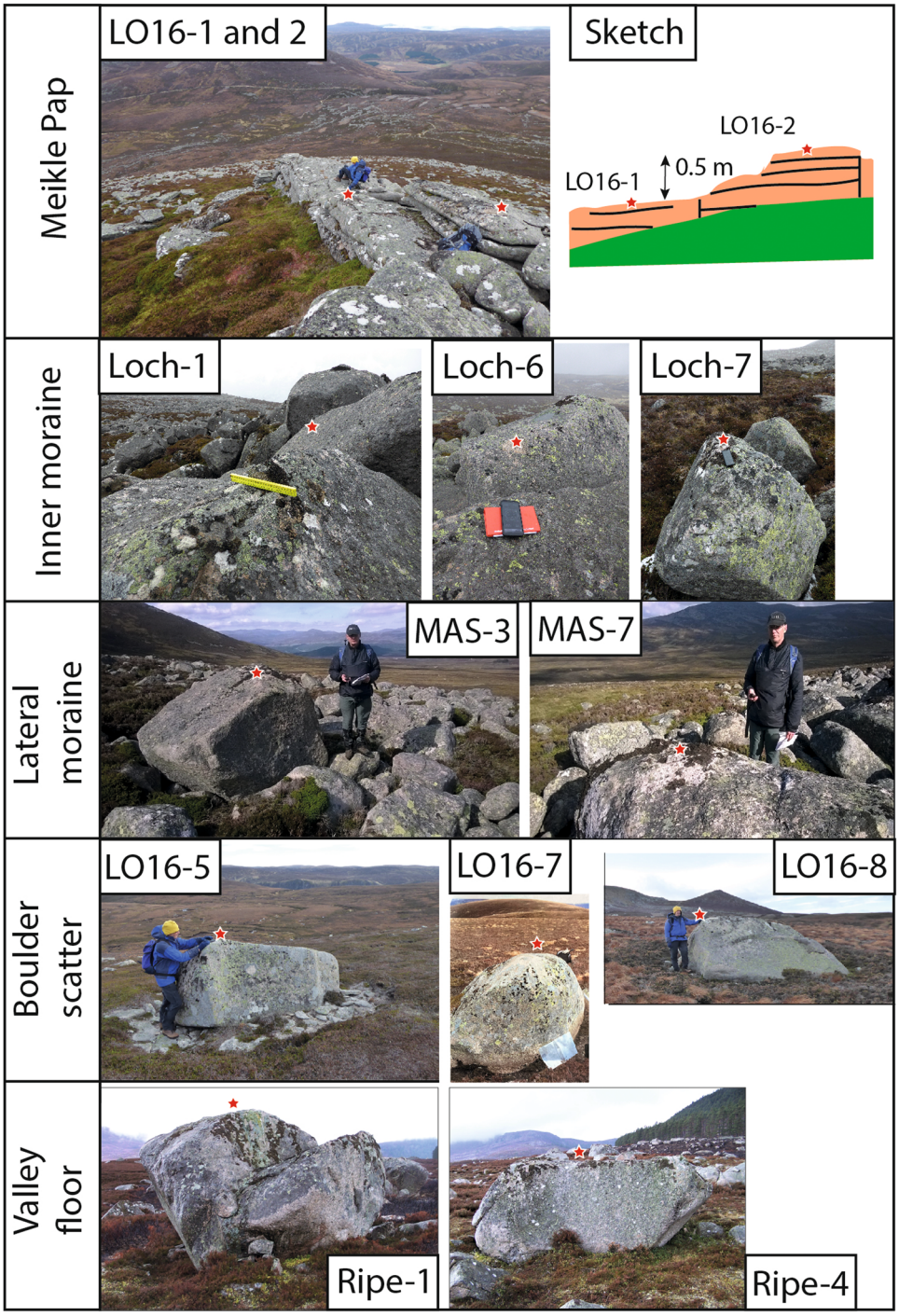


**Figure 4.** Some of the rock surfaces and boulders sampled for TCNs in different domains. [Color figure can be viewed at wileyonlinelibrary.com]

and from the lower tiers of tors from which blocks have been removed by glacial erosion. One erratic boulder age (BB: 15.1 ± 1.2 ka) and two inheritance-corrected ages from transported and rotated tor blocks (CA-1 and MCB-2) constrain the likely deglaciation age for the Cairngorm plateau to 15.6 ± 0.9 ka (Phillips et al., 2006).

In the corrie domain in the Cairngorms, published $^{10}$Be ages for boulder moraines at Coire an't Lochain are 11.5–14.4 ka (Kirkbride et al., 2014), re-calculated here to 12.2–15.3 ka. Assuming Younger Dryas deglaciation at 12.0 ka, maximum measured TCN inheritance is low (<3.3 ka). In the strath domain on the flanks of the northern Cairngorms, boulders probably sourced from the Northern Corries rest on lateral moraines at 540–720 m (Hall et al., 2016). Published $^{10}$Be boulder ages are clustered around 15.1 ka, re-calculated here to 15.3 ka. TCN inheritance is low except for one boulder (CG14-001: 24 ka). Interestingly, the three youngest boulders have a mean age of 14.5 ka that is indistinguishable within error from the expected deglaciation age of 14.7 ka. Compared to Lochnagar, the ages for corrie and lateral boulder moraines in the northern Cairngorms are more strongly clustered and TCN inheritance is lower.

## Discussion

Our initial hope was that we could use cosmogenic nuclides to constrain the timing of the last phase of deglaciation in a part of Scotland where the landform record is clear and has been accepted by different authors over many years. However, many TCN apparent exposure ages at Lochnagar exceeded

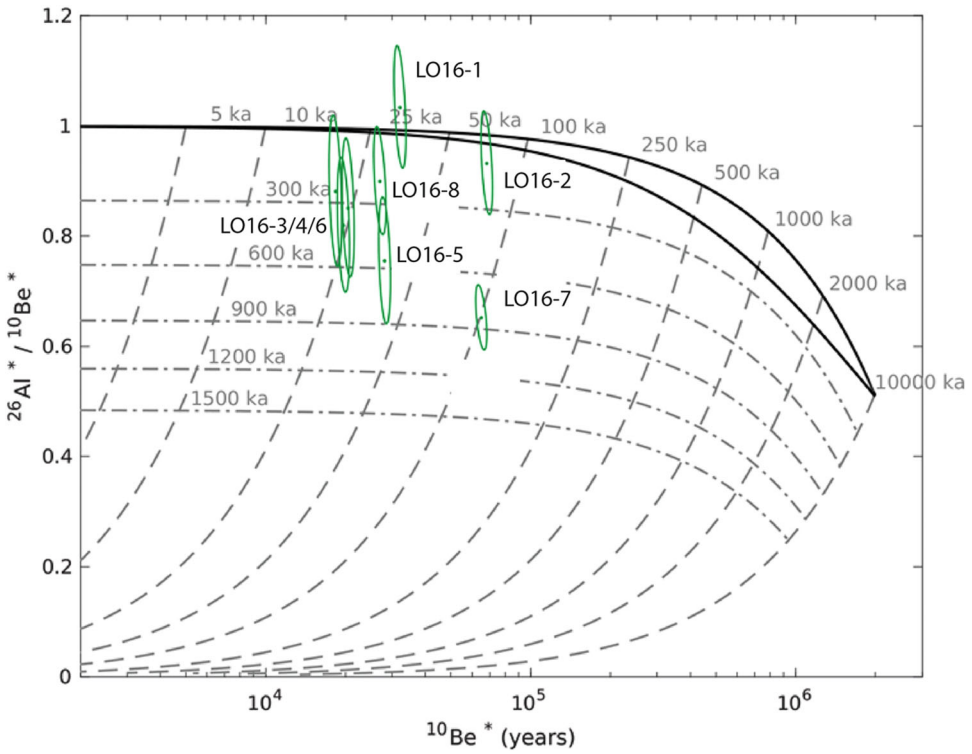


**Figure 5.** Banana plot for $^{26}Al$ and $^{10}Be$ samples LO16-1 to -8. This plot was computed with the iceTEA tool (http://ice-tea.org). Boulders LO-16-3 to -8 have complex exposure histories, including long periods of burial. [Color figure can be viewed at wileyonlinelibrary.com]


**Figure 6.** Distribution of $^{10}Be$ TCN ages for different domains at Lochnagar and in the Cairngorms. Unpublished TCN ages for Lochnagar are indicated by blue circles; previously published ages are shown as orange circles. [Color figure can be viewed at wileyonlinelibrary.com]

expected ages, indicating widespread nuclide inheritance. Below we explore the sources of this inheritance.

## *Exposure and burial history of landscape domains*

The conceptual model of ice cover provides a first-order approximation of a more complex actual chronology, but it is helpful in thinking about the role of prior exposure in the cosmogenic isotope record (Kleman et al., 2020). For the period 122–10 ka, the modelled timing and duration of exposure and burial vary between landscape domains (Fig. 7). The Lochnagar plateau has ice cover for ~66 ka and is ice-free but probably partly snow-covered for ~44 ka (Table 4). In the case of Lochnagar corrie, there is a short period of ice occupation in the Younger Dryas. Importantly, this is only one phase of a possible eight during the last glacial cycle; there were likely to have been several corrie glaciations in MIS 3 (33–57 ka) and several more in MIS 5 (71–110 ka). The total duration of corrie glaciation is 47 ka, with further burial beneath ice sheets and ice fields for 49 ka, and with ice-free conditions restricted to 16 ka of the last 122 ka. The implication is that in the case of Lochnagar corrie there were limited ice-free intervals and thus little time for exposure, reducing the potential for significant TCN inheritance. In the strath domain, conditions suitable for a full ice sheet cover occurred at 15–32 and at 62–75 ka, preceded by a long period of exposure of ~50 ka, perhaps interrupted by 10 ka of

ice cover. The timing and duration of exposure were probably similar in the upper and lower parts of the strath domain as ice thinning by 200 m was rapid (<1 ka) during the last deglaciation in the similar setting of Strath Spey in the northern Cairngorms (Hall et al., 2016). We can assume that variability in ice cover between landscape domains characterized previous glacial cycles and was typical for the wider Cairngorms.

The largest TCN inventories are from exposed bedrock surfaces and boulders in the plateau domain. Published TCN inventories on the Cairngorm plateau show that the greatest apparent exposure ages are from large (>10-m-high) tors. In one case, Clach na Gnuis, combined $^{10}$Be and $^{26}$Al isotopes indicate an exposure and burial history of 626 ka (Phillips et al., 2006), consistent with the advanced development of weathering microforms (Hall and Phillips, 2006b). Large Cairngorm tors have been exposed through multiple glacial cycles and significant parts of their TCN inventories accumulated before the last glacial cycle. The small tor at Meikle Pap near Lochnagar carries a TCN inventory equivalent to 60.9 ka of exposure (LO16-2), like many small tors in the Cairngorms (Fig. 6) (Phillips et al., 2006). For the Meikle Pap tor, after allowing for 15 ka of exposure since the last deglaciation, then the undisturbed tor surface was exposed for the order of 46 ka before being covered by the last ice sheet. The most likely explanation of its apparent exposure age is that the tor was already exposed during MIS 5e (110–125 ka); $^{26}$Al concentrations suggest the tor may have received significant exposure even earlier.

**Table 4.** Estimated burial and exposure history in the landscape domains during the last glacial cycle.

| Domain | Ice cover (ka) | Ice free (ka) |
|---|---|---|
| Plateau | 66 | 46 |
| Corrie | 96 | 16 |
| Strath upper | 36 | 76 |
| Strath lower | 41 | 71 |

In Lochnagar Corrie, two sets of moraines occur (Figs. 1 and 3D). Edge rounding of granite boulders is significantly lower for the inner moraines than for the outer moraines, suggesting that the outer set is older (Kirkbride, 2006). The inner set of moraines at Lochnagar has three sampled boulders with inherited $^{10}$Be nuclide concentrations equivalent to 0.5–4.0 ka of exposure prior to GS-1 (the Younger Dryas). The preceding Greenland Interstadial-1 (GI-1) had a total duration of 1.75 ka, with brief cooling episodes of 0.34 ka total duration during GI-1b and GI-1d (Older Dryas) (Rasmussen et al., 2014). The combined duration of warmer episodes in GI-1a and c was up to 1.4 ka but provided sufficient time for accumulation of only part of the inherited nuclide concentrations (Fig. 7). Moreover, boulders on the lateral moraine were also originally sourced from the corrie. These boulders carry inherited $^{10}$Be nuclide concentrations that are equivalent to 1.6–11.4 ka of additional exposure, with the oldest apparent ages indicating that some boulders were buried beneath the last ice sheet. TCN inheritance in Lochnagar corrie is significantly greater than in Coire an't Lochain in the northern Cairngorms (Kirkbride et al., 2014) (Fig. 6).

High but variable TCN inheritance equivalent to 1.5–43.4 ka of exposure is also present on boulders scattered above the ice-sheet lateral moraine in the upper strath domain (Fig. 1). Here also boulders are interpreted to have survived cover by the last ice sheet. One boulder (LO16-7) has an apparent age of 58.5 ka equivalent to that of the Meikle Pap tor, suggesting ice cover in MIS 6, 4 and 2. A complex exposure and burial history is consistent with the difference of ~20 ka in the $^{10}$Be and $^{26}$Al ages (Fig. 7). We find that the last overriding ice sheet

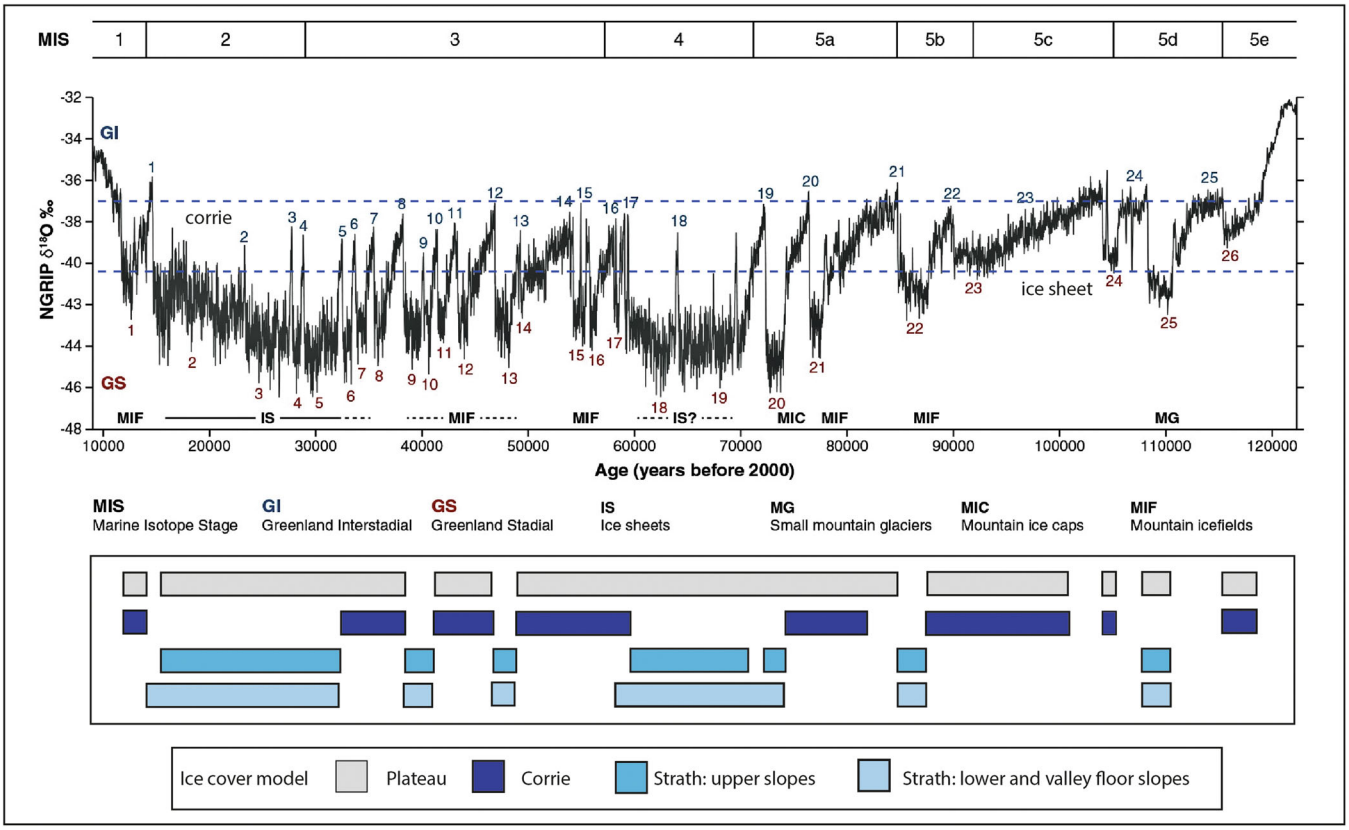


**Figure 7.** A conceptual model of the glacier record in eastern Scotland over the last 122 ka inferred from Greenland ice cores, after Merritt et al. (2019). The thresholds for corrie and ice-sheet glaciation are taken from Clapperton (1997). [Color figure can be viewed at wileyonlinelibrary.com]

in the upper strath domain has recycled boulders with varying degrees of prior exposure, mainly accumulated during the last glacial cycle. The sample boulders were transported for <0.3 km east of the corrie mouth at the time of lateral moraine formation and for distances <3 km from the corrie forefield during earlier phases of glacial transport.

Given the shorter half-life and thus shorter memory for previous exposure we would expect $^{14}C$ ages to be similar to, or younger than, their $^{10}Be$ and $^{26}Al$ counterparts from the same sample. Several samples are reported by the online calculator as being saturated with respect to $^{14}C$, despite $^{10}Be$ or $^{26}Al$ ages that are less than what we might assume for $^{14}C$ saturation. For example, sample LO16-8 has a $^{10}Be$ age of 16.2 ka but is saturated with regard to $^{14}C$. However, the substantially greater external uncertainties for the $^{14}C$ age results provided by the online calculator of Balco et al. (2008) (Table 2) as compared to the internal estimates highlight the uncertainties associated with the $^{14}C$ production rate and consequently the difficulty in assigning $^{14}C$ ages to samples that are older than a few half-lives of $^{14}C$. Assuming concentration uncertainties of 5%, for example, would mean it is difficult to differentiate saturated $^{14}C$ samples from those with an age of ~18 ka. Thus, while the $^{14}C$ ages are reported as being at or close to saturation, apparent discrepancies between the $^{14}C$ and $^{10}Be$, or $^{26}Al$, data are difficult to resolve without better understanding of the uncertainties associated with the $^{14}C$ production rate.

## Bedrock erosion histories

Bedrock erosion through time at Lochnagar represents a balance between weathering and erosion in ice-free periods and glacial erosion during periods of ice-cover. In the plateau domain, ice was generally below its pressure melting point and remained cold-based. Glacial erosion was restricted to block removal from upstanding tors, as at Meikle Pap, to stripping of mountain top detritus, for example above the glacial trimlines at Lochnagar, and to partial removal of blockfields, as on parts of the Cairngorm plateau (Hall and Phillips, 2006b). Consequently, during the last and earlier glacial cycles, erosion of many bedrock surfaces was dominated by slow, steady erosion by granular disaggregation or spalling of small blocks under periglacial conditions. The accumulation of TCN inventories on such rock surfaces then becomes a sum of the cosmic ray flux through time minus surface erosion in ice-free periods and slow nuclide decay during ice burial (Small et al., 1997, Lal, 1991). TCN inventories are highest for the larger tors because of longer exposure of tor summits at or near the ground surface and slow rock surface erosion rates, providing net gains of TCNs during successive ice-free periods.

In the corrie domain, TCN inventories in rock surfaces are expected to be low due to shielding of the corrie walls and to high erosion rates from rock fall (Hilger et al., 2019). Boulder volumes in the Lochnagar moraines provide constraints on erosion rates. The volume of rock debris in the Younger Dryas inner moraines translates to a rate of cliff retreat of ~1.0 m $ka^{-1}$ (Table 5). This estimate is of similar order to rock wall retreat rates of 1.6–3.8 m $ka^{-1}$ in Scotland in this stadial (Ballantyne, 2019). The volume of granite boulders in the outer moraine ridges is between two and three times larger than in the Younger Dryas moraines. Application of the Younger Dryas headwall retreat rate suggests that a total of ~400 ka of active glaciation was necessary for erosion of Lochnagar Corrie. Hence, in common with many cirques (Ruszkiczay-Rüdiger et al., 2021, Crest et al., 2017, Wallick and Principato, 2020), erosion of the Lochnagar Corrie was incremental through multiple Pleistocene glaciations.

At the upper boundary of the strath domain, solifluction lobes terminate downslope at lateral moraines that represent glacial trimlines. Below the lateral moraines, rock is poorly exposed due to a widespread, thin boulder till cover, but hill tops retain tor stumps, for example at Conachraig (Hall, 2007) (Fig. 1). Weak glacial erosion is consistent with advance of a slow-moving ice lobe across the flanks of Lochnagar and earlier cold-based ice cover. The late pulse of erosion and the formation of boulder till may have been triggered by the availability of meltwater as the lobe thinned. This suggestion is supported by the series of ~20 subparallel meltwater channels found at 810–700 m a.s.l. that follow the former surface profile of the ice lobe at gradients of ~150 m $km^{-1}$ (Fig. 3E). Meltwater flowed along the ice margin, suggesting that the ice was cold-based (Johansson, 2007). On the assumption that each channel formed in a single melt season (Mannerfelt, 1945, Seppälä, 2005, Romundset et al., 2023), the ice surface ablated rapidly at 5.5 m $a^{-1}$. Limited glacial erosion and a short duration for transport is consistent with the presence of boulders with inherited TCNs sourced from Lochnagar corrie.

On the lower slopes of the strath domain, below ~550 m a.s.l. and towards the Dee valley floor, more intense glacial erosion through multiple glaciations is indicated by weak streamlining in cols, extensive glacial roughening and the development of large roches moutonnées (Fig. 1). At Ripe Hill, four boulders in a boulder train sourced from a lee side cliff show limited TCN inheritance with a mean age of 13.8 ka, indistinguishable within errors from the minimum 14.6 ka estimate of deglaciation of the Dee Valley based on $^{14}C$ dating of organic remains (Huntley, 1994). This is consistent with low concentrations of TCNs on the source bedrock surfaces after significant glacial erosion through the last glaciation. Here also, the entrainment of a significant number of boulders occurred during the last stages of deglaciation (Sugden et al., 2019).

The overall effects of complex burial, exposure and erosion histories is that today TCN inventories vary widely for rock and boulder surfaces between and within the different landscape domains at Lochnagar and in the wider Cairngorms. The sources of TCN variability from different landscape domains and landforms is shown schematically for blocks A–M in Fig. 8. The present distribution of TCN inheritance within domains and for individual landforms probably resembles that in past interglacial and interstadial periods. This allows the present distribution of TCNs to be used as a proxy for TCN inventories at the start of the last glacial cycle or the onset of the last ice sheet glaciation in MIS 3.

**Table 5.** Volumes of boulders in the Lochnagar moraines.

| Estimate | | Inner moraines | Outer moraines |
|---|---|---|---|
| Cliff catchment area | $km^2$ | 0.39 | 0.39 |
| Boulder area | $km^2$ | 0.46 | 1.2 |
| Boulder depth | m | 2 | 2 |
| Porosity | | 0.5 | 0.5 |
| Boulder volume | $km^3$ | 0.00046 | 0.0012 |
| | $m^3$ | 460 000 | 1200 000 |
| Duration | ka | 1.2 | |
| Boulder creation rate | $m^3\ ka^{-1}$ | 383 333 | |
| Rock wall retreat | m $ka^{-1}$ | 0.98 | |
| Depth of corrie | m | 400 | |
| Time for headward retreat | ka | 407 | |

## Boulder transport scenarios

*In situ* rock blocks have their highest TCN inventories on upper surfaces. TCN inventories decrease exponentially with depth,

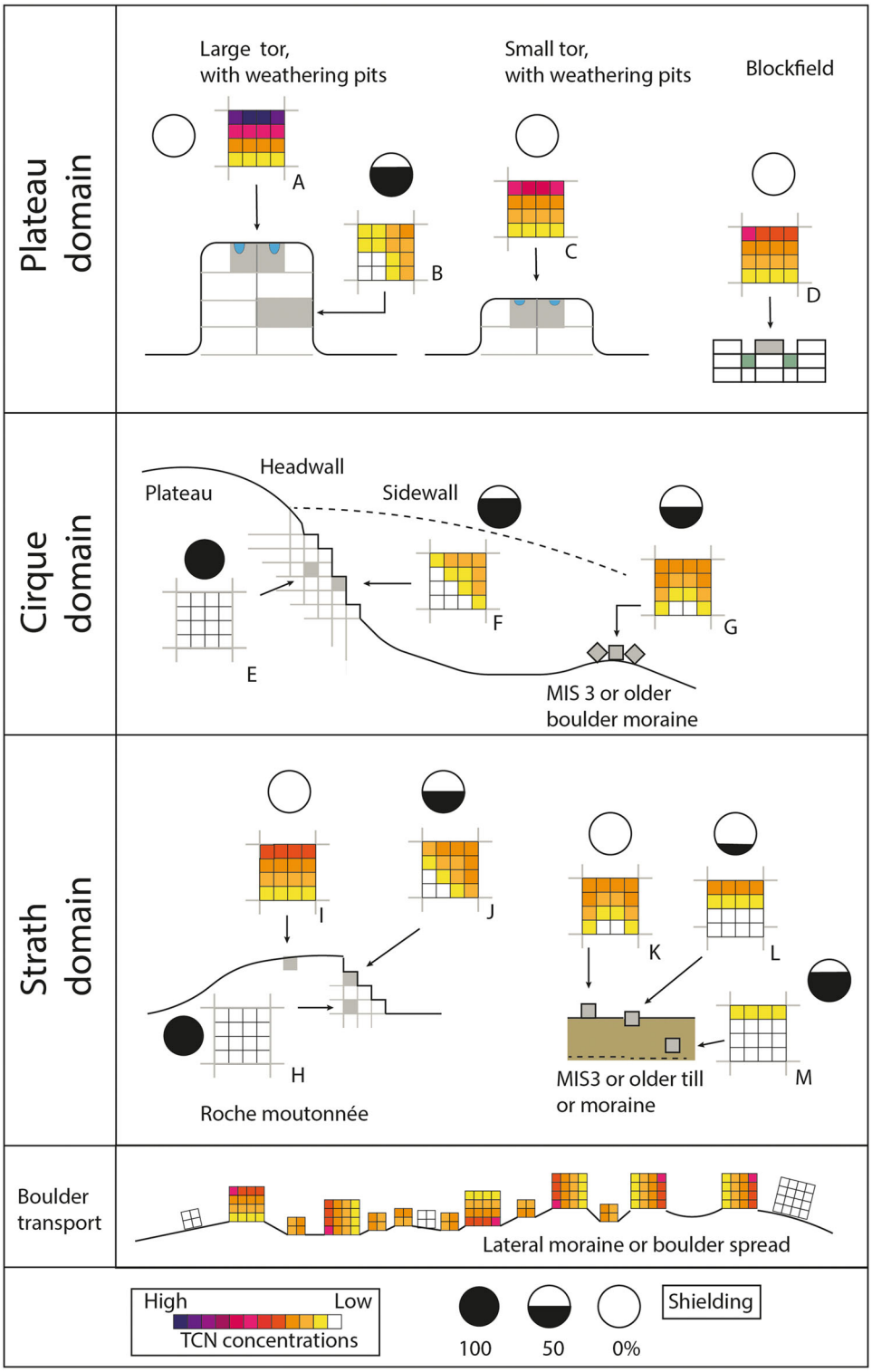


**Figure 8.** Model of TCN inheritance for boulders sourced from characteristic landforms in different landscape domains. Theoretical TCN inventories are shown for 2-m-diameter cubic blocks in the present interglacial based on results from Lochnagar and the Cairngorms. Topographic shielding is indicated. The lower panel shows a schematic model of the potential complexity of TCN inheritance in boulders from the lateral moraine and boulder spread at Lochnagar. [Color figure can be viewed at wileyonlinelibrary.com]

a result of effective cosmic ray attenuation thickness. If the block is >2.5 m in thickness, then at its base self-shielding restricts TCN inventories to small concentrations mainly derived from muogenic radiation (Fabel et al., 2004, Briner et al., 2016). On an upstanding or projecting rock block, for example on a tor or cliff, different block faces may have different inventories due to self-shielding. Also, these inventories may vary across each face of a block (Fig. 8).

When a cubic, jointed-bounded granite block becomes a boulder after its extraction from its bedrock socket, its six faces already carry different TCN inventories. Boulders may then be rotated during transport. For a cubic boulder there is a one in six chance that the original, exposed and upper surface will return to this position after transport and an equal chance that the lower, shielded horizontal surface is left uppermost. In a mixed population of rotated boulders, four in six boulders can be expected to derive from former vertical block faces with intermediate TCN inventories. Boulders also may be split and edge-rounded through abrasion during transport (Carling, 2023). The effect of simple splitting is to make two

smaller boulders. The new faces are from the former interior of the boulder where TCN inventories are relatively low compared to the former top surface but high compared to the former bottom surface of the source block. The effect of abrasion is to remove accumulated TCNs from the boulder surface. The differences in apparent $^{10}$Be exposure ages between zero erosion and 1.6 mm ka$^{-1}$ erosion rates in Table 3 indicate, however, that the effect of abrasion is small. Further complexity develops if boulders are buried (Fig. 8) and recycled through multiple glacial cycles (Zhang et al., 2022) and as boulder corners are reshaped by erosion (Mackey and Lamb, 2013). The overall effect of boulder transport, splitting and surficial erosion in terrain where TCN inheritance is significant is to reduce the probabilities that TCN sampling will include boulders that represent either zero inheritance and so yield reliable deglaciation ages or others that represent maximum TCN inheritance for landforms in the surrounding domain.

In the upper part of the strath domain at Lochnagar the measured boulder populations from the lateral moraine and the boulder spread include (i) one boulder sourced from the plateau domain with a high TCN inventory, (ii) two boulders sourced from Lochnagar corrie with TCN inventories that probably represent only postglacial exposure and (iii) ten boulders with varying TCN inheritance. A significant part of the third variance probably relates to boulder transport effects. The potential complexity of TCN boulder inheritance at Lochnagar in response to boulder sourcing, rotation, splitting and surface erosion is shown schematically in the lower panel in Fig. 8.

## Wider implications

### Problems and potential of TCN inheritance

The original purpose for TCN sampling at Lochnagar was to provide an improved chronology for the wasting of the last Scottish Ice Sheet and its relationship to corrie glaciation in a classic landscape of selective glacial erosion. Our experience here and in the wider Cairngorms indicates that TCN inheritance is widespread and normal in similar plateau and strath domains. Exceptions occur where large blocks have been removed such as from tor stumps (Phillips et al., 2006, Margreth et al., 2016) and the lee faces of rock steps (Phillips et al., 2008). Large and carefully targeted TCN sample sets may be needed to constrain deglaciation ages in these landscapes.

A further complication at Lochnagar is that due to widespread TCN inheritance the mean ages for sample sets represent arbitrary values unrelated to deglaciation ages (Fig. 6). Only the youngest apparent exposure ages on corrie and ice-sheet lateral moraines were close to expected deglaciation ages. In this study, the use of simple statistics, such as means and weighted means, is misleading and more sophisticated statistical processing is inappropriate. Similar difficulties are found in other glaciated terrains with widespread nuclide inheritance in which large datasets confirm that only the youngest exposure ages conform to deglaciation ages (Romundset et al., 2023). More widely, inherited TCNs are common in abraded crystalline bedrock surfaces in lowland parts of Scandinavia (Stroeven et al., 2002, Hall et al., 2019, Briner et al., 2016). Such bedrock sources, together with boulder recycling, may account for many boulder $^{10}$Be ages that exceed expected deglaciation ages below the former Fennoscandian (Stroeven et al., 2016) and Laurentide ice sheets (Halsted et al., 2023).

Whilst TCN inheritance creates difficulties in dating deglaciation, it may also provide opportunities to explore a much longer history of glaciation. In the corrie domain at Lochnagar, inherited TCNs in boulder moraines are consistent with multiple phases of corrie glacier activity and with slow corrie growth, as also suggested by low boulder volumes in Younger Dryas moraines. In the upper strath domain, TCN inheritance records three phases of ice sheet glaciation and the landform record indicates a dominance of cold-based ice cover. In the Cairngorms, the oldest bedrock surfaces on large tors offer potential for depth profiles to extend ice cover histories to beyond 500 ka. Further research is needed in this and similar landscapes to separate (i) exposure and burial from (ii) bedrock erosion histories and (iii) the effects of boulder transportation, disturbance, burial and recycling. This may require establishing the full range and variability of TCN inventories across different landscape domains, on landforms in those domains, and for different nuclides across and at depth within multiple rock and boulder surfaces (Skov et al., 2020, Knudsen et al., 2020, Nørgaard et al., 2023, Andersen et al., 2020).

### Boulder trapping

The accumulation of boulders with a wide range of exposure ages carries a further implication: that the northern flank of Lochnagar has acted as a sediment trap during ice-sheet cycles. Some of the boulders accumulate during corrie glaciations but they are not removed during the following cold-based ice-sheet glaciation. Rather, and specific to the setting, the ice sheet builds up a broad moraine in the mouth of the corrie. The result is an accumulation of ice-sheet sediment containing schist erratics derived from further west that are mixed with local granite.

We propose that the sediment trap on the northern slopes of Lochnagar results from the way nunatak topography can enhance ablation. Topography can create zones of enhanced ablation by concentrating katabatic winds flowing down the surface of the ice sheet (Sugden and Hall, 2020). Such zones are common in the lee of nunataks in the Antarctic Ice Sheet where locally concentrated wind velocities ablate the ice surface to leave a patch of blue or bare ice. The ablation of surface ice at the foot of the mountain causes ice to flow upwards and towards the mountain. In turn, this brings basal and surface debris to the ice margin (Woodward et al., 2022).

Lochnagar is an ideal location for such enhanced ablation and deposition. Katabatic winds would flow down from the main Scottish ice sheet dome in the west and accelerate as they passed over the mountain summit. At such a time, as in West Greenland and Antarctica, the ice-sheet winds would be steered towards the depression in the ice sheet occupied by the Dee valley outlet glacier. The intensity of ablation would increase as the mountain emerged as a nunatak and would be especially important when the relief differential is maximized and yet the ice sheet is sufficiently dynamic to be forming the broad moraine. The result would be to accelerate surface ablation and to cause ice flow and the transport of sediment to the ice margin in the lee of Lochnagar. The sediment is not removed by subsequent ice sheets because they are cold-based. Such a process of accumulation could occur on many different occasions as the ice sheets grew and declined during the Quaternary.

# Conclusion

This paper brings together and reports on two decades of cosmogenic isotope exposure age sampling and analysis at Lochnagar. The northern flank of the mountain holds a clear geomorphological record of corrie glaciation and the thinning

of the last Scottish ice sheet over the last ~15 ka. Four samples from arcuate boulder moraines in Lochnagar corrie yielded $^{10}$Be apparent exposure ages of 10.9–16.0 ka; the expected age is 12.0 ka during GS-1. Seven granite boulders derived from Lochnagar corrie and sampled from a cross-cutting ice sheet lateral moraine yielded apparent $^{10}$Be apparent ages of 14.0–25.8 ka. Six samples from boulder spreads above the lateral moraine yielded apparent $^{10}$Be exposure ages of 16.2–58.1 ka. The expected age of the lateral moraine based on a probable synchronous ice advance in the northern Cairngorms was at the termination of GS-2a at 14.7 ka. On the Dee valley floor, a boulder train yielded $^{10}$Be ages on four boulders of 12.6–15.4 ka, with a mean of 13.8 ka, close to the expected deglaciation age. Hence, three datasets above 600 m a.s.l. have widespread but variable TCN inheritance and each initially appears to be too noisy for reliable attribution of deglaciation ages.

The geological uncertainty implicit in variable inheritance derives from the different histories for rock exposure, burial and erosion across landscape domains and landforms, and different scenarios for boulder transport and erosion. Our results have illustrated how difficult it is to date the timing of the last deglaciation in such settings. The pattern of inheritance varies from place to place and from boulder to boulder. Under these circumstances, the use of means and other statistics is potentially misleading. Indeed, an investigator of the age of deglaciation is forced into the situation of leaning on the youngest exposure ages and viewing all older apparent ages as influenced by nuclide inheritance. The northern flanks of Lochnagar have acted as a sediment trap for glacial deposition for the last two Scottish ice sheets and probably much longer. Our work confirms that the landscapes at Lochnagar and in the wider Cairngorms, like many other plateau domains in areas of former glaciation, have been shaped over long time periods and through multiple glacial, interstadial and interglacial periods through the Middle and Late Pleistocene.

*Acknowledgements.* This paper reports results for TCN samples (Loch- and MAS-) that were collected in 2003 and prepared for AMS by Bill Phillips at the University of Edinburgh. The paper has benefitted from the helpful critical comments of reviewers, Jason Briner and Chris Halsted, and from the review editor, Achim Brauer.

### *Data availability statement*

The data that supports the findings of this study are available in the supplementary material of this article.

## Supporting information

Additional supporting information can be found in the online version of this article.

**Table S1.** Raw data required for calculating nuclide concentrations.

*Abbreviations.* AMS, accelerator mass spectrometry; GI, Greenland Interstadial; GS, Greenland Stadial; TCN, terrestrial cosmogenic nuclide.

## References

Andersen, J.L., Egholm, D.L., Olsen, J., Larsen, N.K. & Knudsen, M.F. (2020) Topographical evolution and glaciation history of South Greenland constrained by paired $^{26}$Al/$^{10}$Be nuclides. *Earth and Planetary Science Letters*, 542, 116300.

Applegate, P.J., Urban, N.M., Keller, K., Lowell, T.V., Laabs, B.J.C., Kelly, M.A. et al. (2012) Improved moraine age interpretations through explicit matching of geomorphic process models to cosmogenic nuclide measurements from single landforms. *Quaternary Research*, 77, 293–304.

Applegate, P.J., Urban, N.M., Laabs, B.J.C., Keller, K. & Alley, R.B. (2010) Modeling the statistical distributions of cosmogenic exposure dates from moraines. *Geoscientific Model Development*, 3, 293–307.

Balco, G. (2011) Contributions and unrealized potential contributions of cosmogenic-nuclide exposure dating to glacier chronology, 1990–2010. *Quaternary Science Reviews*, 30, 3–27.

Balco, G., Stone, J.O., Lifton, N.A. & Dunai, T.J. (2008) A complete and easily accessible means of calculating surface exposure ages or erosion rates from $^{10}$Be and $^{26}$Al measurements. *Quaternary Geochronology*, 3, 174–195.

Ballantyne, C.K. (2010) A general model of autochthonous blockfield evolution. *Permafrost and Periglacial Processes*, 21, 289–300.

Ballantyne, C.K. (2019) *Scotland's mountain landscapes: a geomorphological perspective*. Dunedin Academic Press Ltd.

Binnie, S.A., Dunai, T.J., Voronina, E., Goral, T., Heinze, S. & Dewald, A. (2015) Separation of Be and Al for AMS using single-step column chromatography. *Nuclear Instruments and Methods in Physics Research Section B: Beam Interactions with Materials and Atoms*, 361, 397–401.

Borchers, B., Marrero, S., Balco, G., Caffee, M., Goehring, B., Lifton, N. et al. (2016) Geological calibration of spallation production rates in the CRONUS-Earth project. *Quaternary Geochronology*, 31, 188–198.

Briner, J.P., Goehring, B.M., Mangerud, J. & Svendsen, J.I. (2016) The deep accumulation of $^{10}$Be at Utsira, southwestern Norway: implications for cosmogenic nuclide exposure dating in peripheral ice sheet landscapes. *Geophysical Research Letters*, 43, 9121–9129.

Briner, J.P., Miller, G.H., Davis, P.T. & Finkel, R.C. (2006) Cosmogenic radionuclides from fiord landscapes support differential erosion by overriding ice sheets. *Geological Society of America bulletin*, 118, 406–420.

Brown, I.M. (1993) Pattern of deglaciation of the last (Late Devensian) Scottish ice sheet: evidence from ice-marginal deposits in the Dee valley, northeast Scotland. *Journal of Quaternary Science*, 8, 235–250.

Carling, P. (2023) Coevolving edge rounding and shape of glacial erratics; the case of Shap granite. *UK. EGUsphere*, 2023, 1–33.

Çiner, A., Sarıkaya, M.A. & Yıldırım, C. (2017) Misleading old age on a young landform? The dilemma of cosmogenic inheritance in surface exposure dating: Moraines vs. rock glaciers. *Quaternary Geochronology*, 42, 76–88.

Clapperton, C.M. (1997) Greenland Ice Cores and North Atlantic Sediments: Implications for the Last Glaciation in Scotland. In: Gordon, J.E., (ed.) *Reflections on the Ice Age in Scotland*. Edinburgh: Scottish Natural Heritage.

Clapperton, C.M. (1986) Glacial geomorphology of northeast Lochnagar. In: Ritchie, W., Stone, J.C. & Mather, A.S., (eds.) *Essays for Professor R. E. H. Mellor*. Aberdeen: University of Aberdeen.

Corbett, L.B., Bierman, P.R. & Rood, D.H. (2016) Constraining multistage exposure-burial scenarios for boulders preserved beneath cold-based glacial ice in Thule, northwest Greenland. *Earth and Planetary Science Letters*, 440, 147–157.

Corbett, L.B., Young, N.E., Bierman, P.R., Briner, J.P., Neumann, T.A., Rood, D.H. et al. (2011) Paired bedrock and boulder $^{10}$Be concentrations resulting from early Holocene ice retreat near Jakobshavn Isfjord, western Greenland. *Quaternary Science Reviews*, 30, 1739–1749.

Crest, Y., Delmas, M., Braucher, R., Gunnell, Y. & Calvet, M. (2017) Cirques have growth spurts during deglacial and interglacial periods: Evidence from $^{10}$Be and $^{26}$Al nuclide inventories in the central and eastern Pyrenees. *Geomorphology*, 278, 60–77.

Davis, P.T., Briner, J.P., Coulthard, R.D., Finkel, R.W. & Miller, G.H. (2006) Preservation of Arctic landscapes overridden by cold-based ice sheets. *Quaternary Research*, 65, 156–163.

Dewald, A., Heinze, S., Jolie, J., Zilges, A., Dunai, T., Rethemeyer, J. et al. (2013) CologneAMS, a dedicated center for accelerator mass spectrometry in Germany. *Nuclear Instruments and Methods in Physics Research Section B: Beam Interactions with Materials and Atoms*, 294, 18–23.

Dortch, J.M., Tomkins, M.D., Saha, S., Murari, M.K., Schoenbohm, L.M. & Curl, D. (2022) A tool for the ages: The Probabilistic

 

Cosmogenic Age Analysis Tool (P-CAAT). *Quaternary Geochronology*, 71, 101323.
Douglass, D., Singer, B., Kaplan, M., Mickelson, D. & Caffee, M. (2006) Cosmogenic nuclide surface exposure dating of boulders on last-glacial and late-glacial moraines, Lago Buenos Aires, Argentina: Interpretive strategies and paleoclimate implications. *Quaternary Geochronology*, 1, 43–58.
Everest, J. & Kubik, P. (2006) The deglaciation of eastern Scotland: cosmogenic $^{10}$Be evidence for a Lateglacial stillstand. *Journal of Quaternary Science*, 21, 95–104.
Fabel, D., Harbor, J., Dahms, D., James, A., Elmore, D., Horn, L. et al. (2004) Spatial patterns of glacial erosion at a valley scale derived from terrestrial cosmogenic $^{10}$Be and $^{26}$Al concentrations in rock. *Annals of the Association of American Geographers*, 94, 241–255.
Fülöp, R.-H., Wacker, L. & Dunai, T.J. (2015) Progress report on a novel in situ $^{14}$C extraction scheme at the University of Cologne. *Nuclear Instruments and Methods in Physics Research Section B: Beam Interactions with Materials and Atoms*, 361, 20–24.
Gordon, J.E. & Brazier, V. (2021) The Cairngorm Mountains. In: Ballantyne, C.K. & Gordon, J.E., (eds.) *Landscapes and Landforms of Scotland*. Cham: Springer International Publishing.
Gosse, J.C. & Phillips, F.M. (2001) Terrestrial in situ cosmogenic nuclides: theory and application. *Quaternary Science Reviews*, 20, 1475–1560.
Hall, A.M., Binnie, S.A., Sugden, D., Dunai, T.J. & Wood, C. (2016) Late readvance and rapid final deglaciation of the last ice sheet in the Grampian Mountains, Scotland. *Journal of Quaternary Science*, 31, 869–878.
Hall, A.M., Ebert, K., Goodfellow, B.W., Hättestrand, C., Heyman, J., Krabbendam, M. et al. (2019) Past and future impact of glacial erosion in Forsmark and Uppland. Svensk Kärnbränslehantering AB.
Hall, A.M. & Gillespie, M.R. (2016) Fracture controls on valley persistence: the Cairngorm Granite pluton, Scotland. *International Journal of Earth Sciences*, 106, 2203–2219.
Hall, A.M. & Glasser, N.F. (2003) Reconstructing the basal thermal regime of an ice stream in a landscape of selective linear erosion: Glen Avon, Cairngorm Mountains, Scotland. *Boreas*, 32, 191–207.
Hall, A.M. & Phillips, W.M. (2006a) Glacial modification of granite tors in the Cairngorms, Scotland. *Journal of Quaternary Science*, 21, 811–830.
Hall, A.M. & Phillips, W.M. (2006b) Weathering pits as indicators of the relative age of granite surfaces in the Cairngorm Mountains, Scotland. *Geografiska Annaler*, 88A, 135–150.
Hall, A.M. (2007) The shaping of Lochnagar: pre-glacial, glacial and post-glacial processes. In: Rose, N., (ed.) *Lochnagar: The natural history of a mountain lake*. Dordrecht: Springer.
Halsted, C.T., Shakun, J.D., Davis, P.T., Bierman, P.R., Corbett, L.B., & Koester, A.J. (October 12–14, 2018) Mount Greylock as a cosmogenic nuclide dipstick to determine the timing and rate of southeastern Laurentide Ice Sheet thinning. In: Grove, T. & Mango, H., (eds.). *Guidebook for field trips in New York and Vermont. New England Intercollegiate Geological Conference, 110th Annual Meeting and New York State Geological Association, 90th Annual Meeting*, vol. C4-1. Lake George, New York. pp. 269–290.
Hein, A.S., Fogwill, C.J., Sugden, D.E. & Xu, S. (2014) Geological scatter of cosmogenic-nuclide exposure ages in the Shackleton Range, Antarctica: Implications for glacial history. *Quaternary Geochronology*, 19, 52–66.
Heyman, J., Stroeven, A.P., Harbor, J.M. & Caffee, M.W. (2011) Too young or too old: Evaluating cosmogenic exposure dating based on an analysis of compiled boulder exposure ages. *Earth and Planetary Science Letters*, 302, 71–80.
Hilger, P., Gosse, J.C. & Hermanns, R.L. (2019) How significant is inheritance when dating rockslide boulders with terrestrial cosmogenic nuclide dating?—a case study of an historic event. *Landslides*, 16, 729–738.
Hughes, P.D., Clark, C.D., Gibbard, P.L., Glasser, N.F. & Tomkins, M.D. (2022) Chapter 53 - Britain and Ireland: glacial landforms from the Last Glacial Maximum. In: Palacios, D., Hughes, P.D., García-Ruiz, J.M. & Andrés, N., (eds.) *European Glacial Landscapes*. Elsevier.
Huntley, B. (1994) Late Devensian and Holocene palaeoecology and palaeoenvironments of the Morrone Birkwoods, Aberdeenshire, Scotland. *Journal of Quaternary Science*, 9, 311–336.
Ivy-Ochs, S., Kerschner, H. & Schlüchter, C. (2007) Cosmogenic nuclides and the dating of Lateglacial and Early Holocene glacier variations: The Alpine perspective. *Quaternary International*, 164-165, 53–63.
Ivy-Ochs, S. & Kober, F. (2008) Surface exposure dating with cosmogenic nuclides. *E&G Quaternary Science Journal*, 57, 179–209.
Jansen, J.D., Knudsen, M.F., Andersen, J.L., Heyman, J. & Egholm, D.L. (2019) Erosion rates in Fennoscandia during the past million years. *Quaternary Science Reviews*, 207, 37–48.
Jena, P.S., Bhushan, R., Sharma, S., Dabhi, A.J., Ajay, S., Raj, H. et al. (2023) $^{10}$Be Exposure Age Dating of Moraine Boulders and Glacially Polished Bedrock Surfaces in Karakoram and Ladakh Ranges, NW Himalaya: Implications in Quaternary Glaciation Studies. *Journal of Geophysical Research: Earth Surface*, 128, e2023JF007216.
Johansson, P. (2007) Late Weichselian deglaciation in Finnish Lapland. *Geological Survey of Finland, Special Paper*, 46, 47–54.
Jones, R.S., Small, D., Cahill, N., Bentley, M.J. & Whitehouse, P.L. (2019) iceTEA: Tools for plotting and analysing cosmogenic-nuclide surface-exposure data from former ice margins. *Quaternary Geochronology*, 51, 72–86.
Kirkbride, M., Everest, J., Benn, D., Gheorghiu, D. & Dawson, A. (2014) Late-Holocene and Younger Dryas glaciers in the northern Cairngorm Mountains, Scotland. *The Holocene*, 24, 141–148.
Kirkbride, M.P. (2008) Boulder edge-roundness as an indicator of relative age: a Lochnagar case study. *Scottish Geographical Journal*, 121, 219–236.
Kirkbride, M.P. (2021) Central and Eastern Grampian Highlands. In: Ballantyne, C.K. & Gordon, J.E., (eds.) *Landscapes and Landforms of Scotland*. Cham: Springer International Publishing.
Kleman, J., Hättestrand, M., Borgström, I., Fabel, D. & Preusser, F. (2021) Age and duration of a MIS 3 interstadial in the Fennoscandian Ice Sheet core area – Implications for ice sheet dynamics. *Quaternary Science Reviews*, 264, 107011.
Kleman, J., Hättestrand, M., Borgström, I., Preusser, F. & Fabel, D. (2020) The Idre marginal moraine – an anchorpoint for Middle and Late Weichselian ice sheet chronology. *Quaternary Science Advances*, 2, 100010.
Knudsen, M.F., Nørgaard, J., Grischott, R., Kober, F., Egholm, D.L., Hansen, T.M. et al. (2020) New cosmogenic nuclide burial-dating model indicates onset of major glaciations in the Alps during Middle Pleistocene Transition. *Earth and Planetary Science Letters*, 549, 116491.
Lal, D. (1991) Cosmic ray labeling of erosion surfaces: in situ nuclide production rates and erosion models. *Earth and Planetary Science Letters*, 104, 424–439.
Larsen, N.K., Søndergaard, A.S., Levy, L.B., Laursen, C.H., Bjørk, A.A., Kjeldsen, K.K. et al. (2021) Cosmogenic nuclide inheritance in Little Ice Age moraines - A case study from Greenland. *Quaternary Geochronology*, 65, 101200.
Li, Y., Harbor, J., Stroeven, A.P., Fabel, D., Kleman, J., Fink, D. et al. (2005) Ice sheet erosion patterns in valley systems in northern Sweden investigated using cosmogenic nuclides. *Earth Surface Processes and Landforms*, 30, 1039–1049.
Lifton, N., Sato, T. & Dunai, T.J. (2014) Scaling in situ cosmogenic nuclide production rates using analytical approximations to atmospheric cosmic-ray fluxes. *Earth and Planetary Science Letters*, 386, 149–160.
Mackey, B.H. & Lamb, M.P. (2013) Deciphering boulder mobility and erosion from cosmogenic nuclide exposure dating. *Journal of Geophysical Research: Earth Surface*, 118, 184–197.
Macleod, A., Palmer, A., Lowe, J., Rose, J., Bryant, C. & Merritt, J. (2011) Timing of glacier response to Younger Dryas climatic cooling in Scotland. *Global and Planetary Change*, 79, 264–274.
Mannerfelt, C. (1945) Some Glaciomorphological Forms: and their evidence as to the downwasting of the inland ice in Swedish and Norwegian mountain terrain. *Geografiska Annaler*, 27, 223–228.
Margreth, A., Gosse, J.C. & Dyke, A.S. (2016) Quantification of subaerial and episodic subglacial erosion rates on high latitude upland plateaus: Cumberland Peninsula, Baffin Island, Arctic Canada. *Quaternary Science Reviews*, 133, 108–129.
Merritt, J.W., Hall, A.M., Gordon, J.E. & Connell, E.R. (2019) Late Pleistocene sediments, landforms and events in Scotland: a review of the terrestrial stratigraphic record. *Earth and Environmental Science Transactions of the Royal Society of Edinburgh*, 110, 39–91.

Nørgaard, J., Jansen, J.D., Neuhuber, S., Ruszkiczay-Rüdiger, Z. & Knudsen, M.F. (2023) P–PINI: A cosmogenic nuclide burial dating method for landscapes undergoing non-steady erosion. *Quaternary Geochronology*, 74, 101420.

Phillips, W.M., Hall, A.M., Ballantyne, C.K., Binnie, S., Kubik, P.W. & Freeman, S. (2008) Extent of the last ice sheet in northern Scotland tested with cosmogenic$^{10}$Be exposure ages. *Journal of Quaternary Science*, 23, 101–107.

Phillips, W.M., Hall, A.M., Mottram, R., Fifield, L.K. & Sugden, D.E. (2006) Cosmogenic $^{10}$Be and $^{26}$Al exposure ages of tors and erratics, Cairngorm Mountains, Scotland: Timescales for the development of a classic landscape of selective linear glacial erosion. *Geomorphology*, 73, 222–245.

Putkonen, J. & Swanson, T. (2003) Accuracy of cosmogenic ages for moraines. *Quaternary Research*, 59, 255–261.

Rasmussen, S.O., Bigler, M., Blockley, S.P., Blunier, T., Buchardt, S.L., Clausen, H.B. et al. (2014) A stratigraphic framework for abrupt climatic changes during the Last Glacial period based on three synchronized Greenland ice-core records: refining and extending the INTIMATE event stratigraphy. *Quaternary Science Reviews*, 106, 14–28.

Romundset, A., Akçar, N., Fredin, O., Andersen, J.L., Høgaas, F., Christl, M. et al. (2023) Early Holocene thinning and final demise of the Scandinavian Ice Sheet across the main drainage divide of southern Norway. *Quaternary Science Reviews*, 317, 108274.

Ruszkiczay-Rüdiger, Z., Kern, Z., Urdea, P., Madarász, B. & Braucher, R. (2021) Limited glacial erosion during the last glaciation in mid-latitude cirques (Retezat Mts, Southern Carpathians, Romania). *Geomorphology*, 384, 107719.

Schiffer, M., Stolz, A., López, D.A., Spanier, R., Herb, S., Müller-Gatermann, C. et al. (2020) Method developments for accelerator mass spectrometry at CologneAMS, $^{53}$Mn/$^{3}$He burial dating and ultra-small $^{14}CO_2$ samples. *Global and Planetary Change*, 184, 103053.

Schimmelpfennig, I., Schaefer, J.M., Akçar, N., Ivy-Ochs, S., Finkel, R.C. & Schlüchter, C. (2012) Holocene glacier culminations in the Western Alps and their hemispheric relevance. *Geology*, 40, 891–894.

Seppälä, M. (2005) (ed.) *The Physical Geography of Fennoscandia*. Oxford University Press.

Sissons, J.B. & Grant, A.J.H. (1972) The last glaciers in the Lochnagar area, Aberdeenshire. *Scottish Journal of Geology*, 8, 85–93.

Skov, D.S., Andersen, J.L., Olsen, J., Jacobsen, B.H., Knudsen, M.F., Jansen, J.D. et al. (2020) Constraints from cosmogenic nuclides on the glaciation and erosion history of Dove Bugt, northeast Greenland. *GSA Bulletin*, 132, 2282–2294.

Small, E.E., Anderson, R.S., Repka, J.L. & Finkel, R. (1997) Erosion rates of alpine bedrock summit surfaces deduced from in situ $^{10}$Be and $^{26}$Al. *Earth and Planetary Science Letters*, 150, 413–425.

Standell, M.R. (2014) Lateglacial (Younger Dryas) glaciers and ice-sheet deglaciation in the Cairngorm Mountains, Scotland: glacier reconstructions and their palaeoclimatic implications. Ph.D, Loughborough University.

Steffensen, J.P., Andersen, K.K., Bigler, M., Clausen, H.B., Dahl-Jensen, D., Fischer, H. et al. (2008) High-Resolution Greenland Ice Core Data Show Abrupt Climate Change Happens in Few Years. *Science*, 321, 680–684.

Stone, J.O. (2000) Air pressure and cosmogenic isotope production. *Journal of Geophysical Research: Solid Earth*, 105, 23753–23759.

Stroeven, A.P., Fabel, D., Harbor, J., Hättestrand, C. & Kleman, J. (2002) Quantifying the erosional impact of the Fennoscandian ice sheet in the Torneträsk–Narvik corridor, northern Sweden, based on cosmogenic radionuclide data. *Geografiska Annaler: Series A, Physical Geography*, 84, 275–287.

Stroeven, A.P., Fabel, D., Harbor, J.M., Fink, D., Caffee, M.W. & Dahlgren, T. (2011) Importance of sampling across an assemblage of glacial landforms for interpreting cosmogenic ages of deglaciation. *Quaternary Research*, 76, 148–156.

Stroeven, A.P., Hättestrand, C., Kleman, J., Heyman, J., Fabel, D., Fredin, O. et al. (2016) Deglaciation of Fennoscandia. *Quaternary Science Reviews*, 147, 91–121.

Sugden, D. & Hall, A. (2020) Antarctic blue-ice moraines: Analogue for Northern Hemisphere ice sheets? *Quaternary Science Reviews*, 249, 106620.

Sugden, D.E. (1968) The selectivity of glacial erosion in the Cairngorm Mountains, Scotland. *Transactions of the Institute of British Geographers*, 45, 79–92.

Sugden, D.E. (1969) The age and form of corries in the Cairngorms. *Scottish Geographical Magazine*, 85, 34–46.

Sugden, D.E., Glasser, N. & Clapperton, C.M. (1992) Evolution of large roches moutonnées. *Geografiska Annaler*, 74A, 253–264.

Sugden, D.E., Hall, A.M., Phillips, W.M. & Stewart, M.A. (2019) Plucking enhanced beneath ice sheet margins: evidence from the Grampian Mountains, Scotland. *Geografiska Annaler: Series A, Physical Geography*, 101, 34–44.

Tonkin, T.N. (2022) Schmidt Hammer exposure-age dating of glacial landforms in the Cairngorm Mountains, Scotland. *Zeitschrift für Geomorphologie*, 64, 39–52.

Vasari, Y. & Vasari, A. (1968) Late- and Post-Glacial macrophytic vegetation in the lochs of northern Scotland. *Acta botanica fennicae*, 45, 193–217.

Wallick, K.N. & Principato, S.M. (2020) Quantitative analyses of cirques on the Faroe Islands: Evidence for time transgressive glacier occupation. *Boreas*, 49, 828–840.

Woodward, J., Hein, A.S., Winter, K., Westoby, M.J., Marrero, S.M., Dunning, S.A. et al. (2022) Blue-ice moraines formation in the Heritage Range, West Antarctica: Implications for ice sheet history and climate reconstruction. *Quaternary Science Advances*, 6, 100051.

Zhang, Z., Wang, J., Xu, X., Chang, Z., Cui, H., Liang, Z. et al. (2022) Evidence of glacial erratic rollover revealed by $^{10}$Be and $^{26}$Al concentration variations. *Acta Geologica Sinica - English Edition*, 96, 369–375.